Report No. UT-03.17

GEOFOAM FILL PERFORMANCE MONITORING

DRAFT FINAL REPORT

By: Dawit Negussey
Armin Stuedlein

Geofoam Research Center
Syracuse University

Utah Department of Transportation
Research Division

August 2003

UDOT RESEARCH & DEVELOPMENT REPORT ABSTRACT

1. Report No. UT-03-17	**2. Government Accession No.**	**3. Recipient's Catalog No.**
4. Title and Subtitle Geofoam Fill Performance Monitoring	**5. Report Date** August 2003 **6. Performing Organization Code**	
7. Author(s) Dawit Negussey, Armin W. Stuedlein	**9. Performing Organization Report No.**	
9. Performing Organization Name and Address Geofoam Research Center 239 Hinds Hall Syracuse University Syracuse, NY 13244-1190	**10. Work Unit No.** **11. Contract No.** 01-9003	
12. Sponsoring Agency Name and Address Stan Burns, P.E. Utah Department of Transportation 4501 South 2700 West Salt Lake City, UT 84114-8410	**13. Type of Report and Period Covered** Research from 2000-2003 **14. Sponsoring Agency Code**	

15. Supplementary Notes

UDOT Research Project Managers: Steve Bartlett and Clifton Farnsworth

16. Abstract

The I-15 Reconstruction Project was the first major design-build infrastructure rehabilitation project in the United States. Geofoam offered a novel solution to challenges of settlement and limited time of construction through an urban corridor. The first challenging application that opened the gate of opportunity to install geofoam was the case of the 100 South utility crossing. This report documents the case history of geofoam embankments in terms of this first application. The project background, construction timeline and monitoring results over a period of almost three years are presented. Settlements were observed with magnet extensometers, horizontal inclinometers and level survey. Pressure beneath the geofoam was monitored by total earth pressure cells. The record of monitoring consists of foundation and geofoam fill settlements divided into construction and post construction phases. Most of the geofoam deformation took place during construction. Both during and after construction, settlements of the foundation have been greater than the geofoam deformation. The field results were carefully reviewed to identify temperature and construction related movements. Pressure cell observations indicate the stresses in the foundation beneath the geofoam are of the general order of the working stresses assumed in design.

17. Key Words geofoam, light-weight fill, expanded polystyrene		**18. Distribution Statement** Available: UDOT Research Division Box 148410 Salt Lake City, UT 84114-8410 www.udot.utah.gov/res	
19. Security Classification (of this report) N/A	**20. Security Classification (of this page)** N/A	**21. No. of Pages** 45	**22. Price**

Geofoam Fill Performance Monitoring

Interstate 15 Reconstruction Project

Salt Lake City, Utah

Report To:

UDOT Division of Research and Development
4501 South 2700 West
Salt Lake City, UT, 84119-5998

Att: Clifton Farnsworth
Research Project Manager

Dawit Negussey, Director
Armin W. Stuedlein, Research Assistant
Geofoam Research Center

239 Hinds Hall
Syracuse University
Syracuse, NY 13244-1190
http://geofoam.syr.edu

UDOT Research Contract No. 019003

The authors are responsible for the facts and the accuracy of the information and data presented herein. The content of this report does not necessarily reflect the views or policies of the Utah Department of Transportation or Syracuse University. This report does not constitute a standard, specification, or regulation.

Abstract

The I-15 Reconstruction Project was the first major design-build infrastructure rehabilitation project in the United States. Geofoam offered a novel solution to challenges of settlement and limited time of construction through an urban corridor. The first challenging application that opened the gate of opportunity to install geofoam was the case of the 100 South utility crossing. This report documents the case history of geofoam embankments in terms of this first application. The project background, construction timeline and monitoring results over a period of almost three years are presented. Settlements were observed with magnet extensometers, horizontal inclinometers and level surveys. Pressure beneath the geofoam was monitored by total earth pressure cells. The record of monitoring consists of foundation and geofoam fill settlements divided into construction and post construction phases. Most of the geofoam deformation took place during construction. Both during and after construction, settlements of the foundation have been greater than the geofoam deformation. The field results were carefully reviewed to identify temperature and construction related movements. Pressure cell observations indicate the stresses in the foundation beneath the geofoam are of the general order of the working stresses assumed in design.

Acknowledgments

This project on geofoam applications in the I-15 Reconstruction Project was supported by the Utah Department of Transportation. Steven Bartlett and subsequently Clifton Farnsworth served as research project managers. Their support and assistance with coordination and acquisition of field data is gratefully acknowledged. Terry Meier of Advanced Foam Plastics was instrumental in facilitating the use of geofoam at I-15. Graduate students; Michael Sheeley, Ahmed Elragi, Navaratnam Anasthas, Sundaramoorthy Srirajan, and Xiadong Huang performed tests and analyses. Phillip Burgmeier, Dick Chave, and George Gresovic and specially Patti Ford assisted at various stages of the research and report preparation. The financial support of Huntsman Corporation has been instrumental to sustain the diverse research base and programs of the Geofoam Research Center at Syracuse University.

TABLE OF CONTENTS

1.0 BACKGROUND

1.1. Interstate 15 Alignment

Interstate 15 (I-15) is part of the Eisenhower National Highway System linking Montana, Idaho, Utah, Arizona, Nevada and California. Major cities linked by I-15 include Salt Lake City, Las Vegas, Los Angeles and San Diego. The Utah section of I-15 was built through Salt Lake County in the early 1960's featuring three lanes in both north and south directions. The approximately 400-mile length of I-15 through Utah is the longest stretch of contiguous highway in the state. Salt Lake City has experienced significant growth in the decades following construction of I-15. In more recent years, I-15 has become an important link between NAFTA partners Canada, the United States and Mexico. As a result, total traffic and truck volume have been increasing significantly over the aging I-15 infrastructure.

1.2. The I-15 Reconstruction Project

In the 1980's, UDOT began planning the I-15 Reconstruction Project to correct deteriorating road and bridge conditions and to provide additional capacity around Salt Lake City (FHWA, 2000). The proposed reconstruction included widening 27 km of urban interstate from six to eight general-purpose lanes, with an additional high-occupancy vehicle (HOV) lane and ramp lane in each direction, for a total of 12 lanes. Further, 143 bridges were to be reconstructed or replaced, and an advanced traffic management system was to be implemented to ease congestion at critical segments.

In 1995, Salt Lake City was selected to host the 2002 Winter Olympic Games. To complete the I-15 reconstruction in time for the Olympics, UDOT chose to award the total project to a large consortium. The traditional design / bid / build sequence would have required about nine years. With a stated design / build alternative a consortium of large contractors was to meet a completion deadline well ahead of the Olympics. The design-build contract was awarded in March 1997 to the conglomerate Wasatch Constructors, a joint venture including Peter Kiewit and Sons of Omaha, Nebraska; Granite Construction of Watsonville, California; and Washington Construction of Highland, California (Cho, 1998; and Warne and Downs, 1999).

The I-15 reconstruction alignment, Fig. 1, is within a developed urban setting and cuts across an extensive deposit of compressible sediments. Even where widening of the roadway could be accomplished within available right of way, the time required for surcharging and the magnitude of collateral settlements were judged unacceptable at critical areas. Additional right of way was expensive, yet purchased where essential amounted to almost $50 million by summer of 2000 (FHWA, 2000). Imposed needs to address time, settlement and stability concerns within a restricted right of way encouraged review and implementation of alternative construction methods such as lime cement columns, staged construction with accelerated drainage and the use of EPS geofoam (Negussey, et al., 2001). As alternative construction techniques were being considered, the senior author was invited to introduce engineers from UDOT, consulting firms and contractors to geofoam in April, 1997. Throughout the design and construction, the Geofoam Research Center (GRC) at Syracuse University provided technical assistance, as requested. Former graduate students conducted laboratory tests and analyses. The junior author installed sensors and collected data from the field instrumentation. UDOT collected and transmitted readings to GRC periodically to update and review the performance of the geofoam embankments.

Over 100,000 m^3 of EPS geofoam was used for the I-15 Project and is the largest application to date in the United States (Bartlett, et al. 2001). Construction of

freestanding geofoam wall embankments enabled full use of the available right of way at a pace much faster than construction without surcharging. Wastach Constructors found the geofoam solution to be efficient and cost-effective. The project was completed 6 months ahead of schedule, $32 million under budget with no outstanding claims at the end of the contract. For these and other accomplishments, I-15 received the ASCE 2002 Outstanding Civil Engineering Achievement Award with mention of the innovative use of geofoam as "Styrofoam" in the citation. The geofoam installation at 100 South is the most instrumented and monitored of the geofoam embankments at I-15. The background and performance of the application at this location is presented herein.

1.3. The 100 South Project

Wasatch Constructors identified 100 South Street as a settlement sensitive area. The determining factor for geofoam usage at this site was the presence of critical utility crossings. These included a 406 mm diameter high-pressure gas line, a 900 mm diameter storm sewer and two 1524 mm diameter fiber optic lines. Widening of the I-15 alignment in this area was accomplished with mechanically stabilized earth (MSE) construction and surcharging. The construction method could not be extended over the portion of the utility crossings because the expected settlements of over 1 m were considered unacceptable. The alternatives considered were re-routing the utilities north to the closest overpass structure and back south to link up with the existing line or widening the embankment with geofoam. The re-routing option was estimated to cost about $3 million and would have required a year to complete. Wasatch Constructors elected to widen both the north and southbound directions with geofoam in combination with compacted soil and scoria (lightweight aggregate) fill (Fig. 2). A total of about 6,000 m^3 of geofoam was used at this site, with half of the total per direction. The area in the immediate vicinity of 100 South was neither commercial nor industrial. Concerns for other collateral settlements were minimal and only one house adjacent to the embankment widening had to be purchased.

2.0 SUBSURFACE CONDITIONS

2.1. Geological Setting

Much of Salt Lake City is situated in the northeast quadrant of the Salt Lake Valley, east of the current Great Salt Lake. The Salt Lake Valley, is the eastern-most major basin of the physiographic province called "The Great Basin", which extends from the Wasatch Range westward to the Sierra Nevadas. The basins consist of deep lacustrine, alluvial, and fluvial strata, eroded from neighboring mountains and mostly deposited during the Miocene Epoch, some 5 to 20 million years ago. The Salt Lake Valley is about 40 km long by 26 km wide and is bounded by the Wasatch Range to the east, and the Oquirrh Mountains to the west. The Salt Lake Valley is typical of the Basin and Range province, with north-trending fault block mountains and intervening sediment filled basins (Christensen and Peterson, 1996).

The Great Salt Lake is a shallow sheet of very salty water, from four to eight times as saline as ocean water (compared to the Dead Sea, at ten times the salinity of ocean water), now covers about 5000 square kilometers of a flat, desert intermountain plain at an altitude of about 1280 m (Boutwell, 1933). The Great Salt Lake is the remnant of Lake Bonneville, an extremely large freshwater lake occupying the same region during the Wisconsin Glaciation some 25,000 to 10,000 years ago (Figure 3). The growth of Lake Bonneville and the Wisconsin Glaciation were products of increased precipitation, with the lake growing more or less steadily to its first peak about 17,000 years ago. The level of Lake Bonneville fluctuated several times in the Pleistocene Epoch. The ancient

shorelines are visible in the talus benches along the Wasatch foothills and other minor ranges. The second rise, according to Gilbert (1890), reached the highest level ever, the Bonneville level, after which the lake overflowed and dropped quickly to the lower Provo stage where it was fixed at the outlet by a bedrock barrier for prolonged period (Stokes, 1986). The lake receded to its lowest stage, was then raised to the Stansbury level, and dropped during the recent or Holocene Epoch to form the current Great Salt Lake. The stages of Lake Bonneville to the current Great Salt Lake are shown in Figure 4.

The northern part of the Salt Lake Valley is underlain by lacustrine, marsh, and alluvial Holocene deposits that formed following the drop in the level of Lake Bonneville. The Jordan River flows north through the valley cutting swaths into the lake sediments and leaving deposits of gravels, sands, silts and minor clay. The alluvium in the Jordan flood plain is at most 4 m in thickness and overlies the Lake Bonneville deposits. The dominant and problematic strata along the I-15 corridor are Lake Bonneville deposits and will be discussed in reference to the geofoam application.

2.2. Subsurface Conditions

Cone (CPT) and Standard (SPT) penetration testing together with tube and split-spoon sampling were conducted at various locations along the I-15 Reconstruction corridor. Figure 5 shows a CPT profile for a location near the geofoam embankments at 100 South. The upper 7 m of the profile consist mainly of alluvial silts and sands. The Lake Bonneville clay deposits extend from 7 to 27 m and contain lenses of sand and silt that vary in thickness from millimeters to meters. The lenses do not provide adequate continuity to assist in dissipation of excess pore pressures within the clay layers. The lake deposits at 100 South are considerably more broken up by the interbeds than at other geofoam locations as at 3300 South. The CPT profile terminates in Pleistocene alluvium below 27 m that predate the formation of Lake Bonneville. Groundwater levels typically vary between depths of 2 to 5 m.

The Lake Bonneville clays are of low to medium plasticity, with water contents ranging from 15 to 55%, with representative averages of 30 to 35%. Corresponding plastic and liquid limits generally range from 15 to 35 and 30 to 60, respectively. The liquidity index for the clays range from 0 to 1.5, with representative averages ranging from 0.4 to 0.9. Dry densities of test samples were between 11 to 18 kN/m^3. Typically, the lower range of dry densities correspond to silty clays and the higher dry densities apply to non-plastic silts and sands. Generally, the spread in moisture content values is larger for 100 South compared to other geofoam sites. Corrected N_{60} values for the lake sediments were generally between 4 to 10. Undrained shear strengths based on vane and unconfined compression tests vary between 5 to 100 kPa. Values of moisture content, dry density and shear strengths with depth are shown in Figure 6.

Oedometer tests results indicate the coefficient of consolidation of clay samples vary between 0.01 to 0.1 m^2/day, with an average of about 0.04 m^2/day. Values of strain compression indices for samples obtained near 100 South ranged from 0.05 to 0.34, with a representative average of 0.15. Secondary compression indices vary between 0.001 to 0.01, with typical values of 0.004 obtained from laboratory tests and 0.007 derived from field observations. Settlement data maintained by UDOT from the initial I-15 construction provide further insight into the consolidation characteristics of the Bonneville deposits. Embankments at 100 South of 6.5 and 7.6 m heights have developed settlements of about 1.4 m over 30 years.

3.0 DESIGN CONSIDERATIONS

Type VIII geofoam (ASTM C-578) blocks of 18 kg/m^3 minimum density were installed as manufactured. A series of laboratory tests performed at GRC confirmed the

density of geofoam supplied to the I-15 project exceeded the minimum specified density. The average compressive strength at 10% strain of 110 kPa was also higher than the specified minimum of 90 kPa listed in ASTM-C-578. A design working stress of 30% for dead load and additionally up to 10% of the compressive resistance at 10% strain was allowed for transient loading. This criterion was selected to limit end of construction settlements to less than 1% strain and below 2% strain in a post-construction period of 50 years. The corrected modulus to 1% strain obtained from the laboratory tests were in the range of 3-5 MPa. The laboratory tests were performed on 50 mm cube samples at a strain rate of 10% per minute; as per ASTM-D-1621. According to the new ASTM D 6817 specification standard, the designation for geofoam blocks used for the 100 South embankments is EPS 19. More recent geofoam material property investigations conducted at the Geofoam Research Center have been presented by Sun (1997), Sheeley (2000), Elragi (2000), Anasthas (2001), Srirajan (2001) and Negussey (2002).

4.0 INSTRUMENTATION

4.1. Magnet Extensometers

4.1.1. Introduction

Magnet extensometers have been used to monitor settlement and heave in various geotechnical applications. A test embankment was constructed to failure in Rio de Janeiro with observation by two magnet extensometer columns (Ramalho-Ortigao, 1983). Magnet extensometers were fitted to vertical inclinometer casing along a portion of the Central Artery/Tunnel for monitoring of a tied-back deep excavation (O'Rourke and O'Donnell, 1997). The performance verification of lime-cement columns at this same I-15 Project was based on magnet extensometer observations (Saye, et al., 2001). Magnet plates were installed in the bedding sand below the 100 South geofoam embankment at alternate block layer intervals. The plates were sequenced along a central riser PVC access pipe and move with the surrounding fill.

4.1.2 Instrument Description

The magnet extensometer system used for the 100 South geofoam embankment consists of settlement plates and permanent magnets, PVC riser pipe segments and a sensing probe and measuring tape. Each settlement plate is a square of 305 mm sides and 12.5 mm thickness with an annular permanent magnet collar, of 60 mm outside diameter, fitted at the center. The magnet collar opening is about 34 mm in diameter to accept a schedule 40 PVC pipe of nominal 25 mm inside diameter. The plate and magnet collar assembly slide freely along the stem of the PVC riser pipe to position at the desired level. The dead zone between the north and south poles of the permanent magnet is a narrow section and is fixed relative to the position of the plate. A magnet probe suspended by a graduated tape with conductors is lowered from surface through the PVC pipe to detect the location of the dead zone and thus the position of the attached plate. The depth location from surface to each magnet plate can be read to the 1 mm graduation on the measuring tape, and readings are repeatable to ± 3 mm. Figure 7 shows the depth measuring tape and the magnet probe inserted within a PVC riser pipe. A gas-powered post-hole augur was used to bore through the geofoam blocks at selected locations to accommodate the PVC riser pipe (Figure 8). The geofoam block was then raised and lowered passing the riser pipe through the augured hole (Figure 9). Several settlement plates were nested vertically over the height of one PVC riser pipe and at different elevations within the fill. Plastic sheeting was placed over the final or top magnet plate to provide a bond free interface between the load distribution slab and the underlying geofoam. As the fill settles, the plate positions adjust accordingly. Successive changes in

depth of magnet plate positions in reference to an initial baseline survey represent the rate and amount of movement over a depth profile.

4.2. Horizontal Inclinometers

4.2.1. Introduction

Horizontal inclinometers are used to develop vertical settlement profiles while vertical inclinometers are used to monitor lateral movements in a variety of geotechnical applications (Green and Mikkelsen, 1988). Three large 45-m diameter oil tanks were instrumented with a series of horizontal inclinometers along the Nile delta in Egypt (Hamza, 1994). The inclinometers were intended to provide prior warning of excessive settlements in a plan to avoid failure. Bridge approach embankments at the Delaware and Hudson Canal crossings in Delaware were instrumented with horizontal inclinometers to establish end of primary consolidation settlements in advance of pile-driving (Brylawski, et al., 1994). The results of monitoring showed settlements were overestimated in design, and construction was allowed to proceed early. Horizontal inclinometers were used in the lime-cement column area of the I-15 Reconstruction (Saye, et al., 2001). Results showed that the application was successful in limiting vertical deformations of the widened embankment. Horizontal inclinometers were installed at the 100 South Site at three locations. Two were placed in the bedding sand below the geofoam-widened embankment. The third horizontal inclinometer was placed within the geofoam fill between layers 8.5 and 9.5 and extends across the geofoam embankment into the area of scoria or lightweight aggregate fill.

4.2.2. Instrument Description

The horizontal inclinometer system consists of the sensing probe, cable, slotted casing segments and a readout unit. The casing used is extruded PVC of 85 mm diameter and was supplied in 3.05 m lengths with tongue-and-groove slot-snap connection ends. When installing the casing, the orthogonal sets of grooves were oriented to align in vertical and horizontal. Successive casing segments were linked to the desired length maintaining the slot continuity. Each snap connection has an O-ring seal to prevent soil and water from entering the casing. Access ports were fabricated and placed around each base inclinometer casing opening followed by placement of a concrete headwall that tied into the grade beam. The casings for both base inclinometers of the North and South array are in the leveling course below the geofoam fill. To place the top inclinometer firmly within the geofoam fill, a trench was cut into marked geofoam blocks using a set of plywood forms or templates as guides, Figure 10. The templates were traced with a hot-wire saw to form a continuous trench. The U shaped cut geofoam was removed and geotextile fabric was placed to straddle across block joints. A continuous length of 30.5 m of casing was placed with sand bedding and surrounding from the edge of the fill to about the southbound road way centerline, Figure 11. The access end of the top inclinometer casing (Figure 12) was fixed in place by expandable urethane foam grout. After the required length of casing was placed, a cap and pulley assembly was fitted to the terminal or dead end of the inclinometer casing. A parallel return PVC pipe of 12.5 mm I.D. fits to the end cap system. A 3 mm steel wire runs through the inclinometer casing, over the pulley and back through the return pipe to the access port. Both the base and top horizontal inclinometers were carefully installed in straight and initially level alignment.

The horizontal inclinometer probe uses two servo-accelerometers to measure the angle of tilt. The probe has a wheelbase of 600 mm, a range of +/- 35°, and weighs about 5 kg. The resolution and repeatability, as suggested by the manufacturer, is 0.03 mm per 600 mm and +/- 0.003°, respectively (Slope Indicator, 2002). The probe and readout unit are shown in Figure 13. The procedure for taking readings commenced with surveying of

the top of the casing with reference to an external benchmark. After the survey was completed, the probe was attached to the readout cable and the pull wire to be drawn to the dead end of the inclinometer casing. When the probe reached the end of the casing, the pull cable was retracted in 600 mm decrements to take readings. After a set of readings was obtained, the inclinometer was inverted, and the procedure was repeated. Tilt measurements from the reversed probe were used to cancel errors due to sensor bias and to generate checksums and to validate the survey.

4.3. Stress Cells

4.3.1. Introduction

The use of stress cells has proved valuable in verifying performance and confirming design assumptions in many projects. Problems arise when attempting to make earth pressure measurements because presence of the sensor generally modifies the stress field intended to be measured (Hanna, 1985; Weiler and Kulhawy, 1978). By maintaining a high diameter to thickness aspect ratio, errors arising from soil-cell relative stiffness, diaphragm deflection and arching have been minimized. The Oroville Dam, a large embankment dam on the Feather River in California, was instrumented with earth pressure cells (O'Rourke, 1978). The stress cells allowed identification of problems that possibly lead to hydraulic fracture. A stone column test embankment over soft marine clay was instrumented with total earth pressure cells to determine the portion of load carried by the (Munfakh, 1983). A large geofoam embankment was constructed at the base of Mt. Gassan, Japan, to minimize slope movements during passage of 32-ton haul trucks. The embankment was instrumented with earth pressure cells to verify stress distribution for guidance in setting speed limits for heavy trucks (Arai, et al., 1996). Earth pressure cells were installed at 100 South to observe changes in pressure during construction and under steady loading in the post construction stage. Each of the North and South Arrays has an associated cell pressure within the leveling course below the geofoam fill.

4.3.2 Instrument Description

Stainless steel pressure cells of 345 kPa capacity were used at 100 South. Each stress cell consists of a thick base plate and thin diaphragm welded along the edges to form a 230 mm diameter thin circular cavity. In profile, each stress cell is nominally 6 mm thick. The thin circular cavity contains an incompressible fluid of low freezing temperature, deaired glycol. A stiff stainless steel tube connects the fluid to a vibrating wire transducer away from the cell edge so that the presence of the transducer housing does not affect the pressure registered by the stress cell. Changes in contact pressure over the flexible face of the cell induce movement of a diaphragm in the vibrating wire transducer. The frequency response of the vibrating wire attached to the diaphragm changes in response to the applied pressure. The stress cells have accuracy and resolution ratings of +/- 0.9 kPa and +/- 0.4 kPa, respectively. The stress cell leads run laterally to the face of the fill and alongside the grade beam to an access port. Stress cells are buried at 150 mm depth in the bedding sand below the geofoam fill. Information gathered during cell reading included the vibration frequency and cell temperature. The field readings were then used to calculate stresses based on a calibration relationship for each cell provided by the manufacturer.

4.4. Settlement Survey

4.4.1. Introduction

Optimal surveying methods provide an inexpensive means of performance monitoring and are necessary in instances where subsurface instrumentation are employed to tie into benchmarks. The casings of the horizontal inclinometers and magnet

extensometers have been surveyed periodically since installation. A series of settlement points were established on the grade beam of the fascia wall along a portion of the geofoam wall, transition area to the mechanically-stabilized earth wall, and the south side mechanically-stabilized earth wall. Settlement surveys were conducted with a high precision self-reading level and rod. The self-reading level accuracy is of the order of 0.8 mm standard deviation on a 1 km double-run circuit (Bartlett, et al., 2001). Surveys were referenced to a stable off-site benchmark and were checked for closure.

4.5. Instrumentation Array Layout

The 100 South Street site corresponds to Retaining Wall R351 for the I-15 Reconstruction Project, at stationings shown in Figure 14. The instrumentation at 100 South consists of two distinct arrays, labeled the North Array and the South Array (Figures 14 and 15) all placed in the southbound portion of the embankment. The North Array is located at R351 stationing 1+112 m, and the South Array is located at R351 stationing 1+126 m.

The North Array consists of a magnet extensometer column, located at about 2 m from the edge of fill, together with an adjacent base horizontal inclinometer and stress cell. The horizontal inclinometer is 4.3 m long and ties into the toe of the existing earth embankment. The extensometer array consists of a total of 7 magnet plates including one in the leveling sand below the geofoam and the rest distributed at different layers of the geofoam and load distribution slab interfaces over a total height of about 7.7 m.

The South Array includes a magnet extensometer column, also placed about 2 m from the edge of the fill, two base stress cells, located 1.2 and 2.4 m from the edge of the fill adjacent to the extensometer, and a base and top horizontal inclinometers. The base horizontal inclinometer is 4.9 m long, and ties into the toe of the existing earth embankment. The top inclinometer is 30.5 m long and spans across the west half of the southbound roadway, transitioning from geofoam to new compacted soil and scoria lightweight fill areas. The South extensometer column also consists of 7 magnet plates in the same sequence as the North Array, but the total height is about 7.3 m, as shown in Figure 16.

The riser pipes for both magnet extensometer columns were extended to the pavement grade. To facilitate access and protect the geofoam fill from surface contaminants, a triple casing scheme with flush-mounted monitoring well cover was provided, as shown in Figure 17. In addition to surveying the casings of the magnet extensometer and horizontal inclinometer headers, 18 survey points were established along the grade beam supporting the facia panels starting from about the North Array and extending into the MSE wall section as previously noted. The locations of the grade beam survey points are shown in Figure 15 and the reference numbers and stationing are as following:

Point Number	Stationing
1	1+163.5
2	1+160.3
3	1+157.2
4	1+154.9
5	1+152.9
6	1+150.4
7	1+147.9
8	1+145.4
9	1+143.0
10	1+140.5
11	1+135.6
12	1+130.6
13	1+125.7
14	1+120.7
15	1+115.8
16	1+110.8
17	1+106.0
18	1+103.5

5.0 RESULTS

5.1. Construction Sequence and Load History

The 100 South portion of the southbound interstate served as a ramp to the top of the embankment during construction of the MSE walls. Preparation for the geofoam fill footprint began by excavating a height of subgrade equal to the weight of the pavement structure, in mid July of 2000. PV sand of 300 mm depth was tamped and leveled to a tolerance of +/- 10 mm per 3 m on July 21st (reference day 0). Geofoam placement by work crew of 3 men and an equipment operator began on day 0 and ended on August 4th, day 14 (Figure 18). The load distribution slab was poured on day 24, followed by a 7-day curing break. The majority of pavement sub-base and base, consisting of lightweight (10 kN/m^3) scoria and open graded granular base course was placed in the 8-day period leading up to August 29th. Thereafter, a 200-day construction rest period commenced for other portions of construction to catch up. The 350 mm PCC pavement was poured on March 15th, 2001. The stress level of about 31 kPa at this stage corresponds to 30% of the 110 kPa compressive strength at 10% strain obtained from testing geofoam samples supplied to the project. Final detailing of the interstate at 100 South took about 60 days at which time a jersey barrier and planter box were poured, the planter box was filled, and the sound barrier was erected. Construction was completed in mid May after about 10 months. The additional stress of about 10 kPa associated with the final detailing loads at the edge of the roadway does not represent average stress levels over most of the geofoam fill.

5.2. Deformation Performance

The deformation performance of the 100 South geofoam embankment was observed by means of magnet extensometer columns, horizontal inclinometers, and a foundation settlement survey as described in Section 4. The performance of the fill is described in terms of construction related deformations and post-construction settlements. Base horizontal inclinometer observations and the settlement surveys represent

foundation settlements. The difference between top and base horizontal inclinometers and magnet extensometer observations indicate settlement of the geofoam mass. The top inclinometer also provides a profile of settlements involving the geofoam fill; compacted soil and scoria fill over the existing embankment.

Reference day 0 of the construction timeline corresponds to the baseline reading of the base stress cells on July 21, 2000. Deformation observations at 100 South began on July 17, with baseline readings of the North base inclinometer. Initial South base inclinometer readings were taken on July 20. Baseline magnet extensometer readings were taken on August 8th after the geofoam blocks were installed. Correspondingly, the baseline of the magnet extensometers, and therefore the record of the geofoam settlement readings by extensometer observations began on day 18 and before pouring of the load distribution slab. The baseline reading for the top inclinometer was taken on August 29, or day 39, after placement of the load distribution slab and road base. The elevation survey along the grade beam foundation of the fascia panels was taken in September 2001 and thus subsequent observations represent post construction foundation settlements. These differences in start time and construction activity before the respective baseline readings should be noted, specially, when comparing construction stage settlements.

5.2.1. Construction Stage Settlements

Figures 19 and 20 show construction stage foundation settlements below the geofoam embankment derived from the North and South base inclinometer observations, respectively. For each profile, the settlements shown are with respect to the corresponding baseline survey, also shown in the same Figure as the initial elevation profile. Initially, settlement profiles for both base inclinometers indicate more settlement at the back or dead end. As construction progressed, the front or open end began to settle more. By the end of construction, a total of about 80 mm foundation settlement was registered at both the North and South base inclinometers. The base inclinometer profiles indicated a slight cross slope of about 0.2 percent towards the roadway centerline. The North base inclinometer profile was relatively level but became inaccessible after July 2001. Foundation settlement observations below the full height geofoam fill by the two base inclinometers during the construction period were in very good agreement in trend and magnitude.

Construction stage settlement of the geofoam fill was observed with magnet extensometers at layers 0, 1.5, 3.5, 5.5, 7.5, 8.5 and 9.5 at the North array, and layers 0, 1.5, 3.5, 5.5, 7.5, 8.5, and 9 at the South array. All extensometer observations are in reference to the respective base plate underlying the geofoam fill (and not the top of the riser pipe) and represent deformations of the geofoam fill over time. Figures 21 and 22 show the construction settlement time history for the North and South array, respectively, in terms of cumulative layer deformations. Settlements observed on day 26 due to installation of the load distribution slab ranged from 3 to 6 mm per instrumented layer of two blocks height intervals of the North array. The total settlement for the full geofoam height was 21 mm. Corresponding interval settlements for the South array varied between 3 to 5 mm, with a total settlement of 22 mm. Placement of the scoria sub-base and open graded base ended on August 29th. Geofoam settlements continued during the construction rest period and gradually slowed. Readings taken on day 109 indicate total settlements of 61 and 66 mm for the North and South array, respectively. Construction resumed after delay for other activities to catch up and the PCC pavement was poured on March 15, 2001; day 237. Installation of jersey barriers, planter boxes, and sound barrier walls was completed by middle of May, 2001. Total settlements by the end of construction and opening for traffic amounted to 75 and 80 mm for the North and South array, respectively. Figures 23 and 24 show the construction strain time history derived

from the extensometer observations. The bottom 1.5 layers show about 1.4 and 1.8 percent strain by end of construction. The cumulative strain throughout overlying geofoam fill layers was relatively uniform. The average cumulative strain at the end of construction for both the North and South arrays was about 1 percent, as previously anticipated in design.

Figure 25 shows the total settlement profile across the new and old embankment based on observations of the top inclinometer. At the end of construction, referenced as September 24th, 2001 about 130 mm and 140 mm of total settlement was observed at the fascia panel and full height geofoam fill segments inward from the face, respectively. End of construction settlements decreased with further distance inward to about 50 mm at the dead end of the slope indicator near the center of the South bound I-15 roadway. These end of construction deformations represent both geofoam fill and foundation settlements. Thus to obtain estimates of the geofoam fill deformations separately, the foundation settlements indicated by the base inclinometers need to be subtracted. However, as the baseline readings of the top and base inclinometers were on different dates and there was prior loading before the top inclinometer was first surveyed; some adjustments had to be made. Stuedlein (2003) estimated initial settlements of the geofoam fill due to the load distribution slab and base course placement from the magnet extensometer records to be about 28 mm. By subtracting the end of construction foundation settlement of 80 mm indicated by the base inclinometers and allowing for the suggested 28 mm adjustment; the end of construction settlement of the geofoam fill can be estimated to be about 85 mm. This estimate is in reasonable agreement with the cumulative end of construction geofoam settlements derived from the magnet extensometer monitoring. Overall, end of construction settlements of the foundation were about equal to the geofoam fill settlement. Results shown in Figure 25 do not include the 28 mm settlement adjustment for different start times.

5.2.2. Post-construction Settlements

The post-construction settlement record at 100 South spans a period of almost 600 days. The frequency of observations had decreased with the end of construction and opening of the roadway to traffic. The observation record has a break of 200 days after which readings were again initiated at closer time intervals to closely monitor and identify the possible cause of the seasonal deformation explained below. Figures 27 and 28 show the cumulative settlement histories of the geofoam fill at the South and North Array, respectively. Post construction settlements of geofoam layer intervals have been less than 5 mm. The total post construction settlement of the geofoam fill to date has been less than 15 mm at both the South and North extensometer arrays. Post-construction strain increments are shown in Figure 29 and 30. Since the end of construction, strains for two geofoam layer intervals between extensometer plates increased by about 0.2 percent to a cumulative strain of about 1.2 percent. At both the North and South extensometer arrays the lowest geofoam layers remain at a higher level of strain than the overlying blocks but below 2 percent.

Figure 31 shows the approximate end of construction and post construction settlements for the base and top horizontal inclinometers. Both at the end of construction and for the post construction profile, foundation settlements were slightly higher at the back end of the inclinometers closer to the position of the new compacted fill. The profiles of the top inclinometer in both construction and post construction phases indicate the casing head and fascia panel positions at the outer face remain higher relative to full height geofoam sections inward. The top inclinometer settlement increment indicates comparable movement at the edge and full height geofoam sections. Post construction settlements decrease with distance toward the roadway centerline and dead end of the top inclinometer. Allowing for the shorter time base of the top inclinometer data in post

construction compared to the interval for the base inclinometer, the post construction deformations in the geofoam fill have been much less than the incremental settlements of the foundation. The design transverse grade of the roadway was 2%. Based on the post construction settlement profile, the maximum change in cross slope to date is likely of the order of only 0.2 percent. The top horizontal inclinometer has been valuable in providing information on differential movements. Future monitoring should include observation of the roadway condition and surface profile as well as the fascia panels.

Figure 32 shows the complete time history of settlements of the horizontal inclinometer casing heads or openings. These settlements are based on optical surveys and cover both the construction and post construction periods. The time axis origin for each profile begins from the respective baseline survey. Initial observation date differences become less significant with time. Observations about post construction performance can be made without attempting initiation time adjustments. The results suggest post construction settlements have been occurring primarily in the foundation and not within the geofoam fill.

5.2.3. Additional Observations

When the magnet extensometer observations were referenced to the top of the riser pipes, a seasonal trend of cyclic deformation became evident. This phenomenon is shown in Figure 33 where changes in depth to base plate from the top of riser pipes have been plotted against time together with corresponding 30 years average daily temperatures for Salt Lake City. Increased depths or apparent more settlement is indicated in Summer months. Decreased depths to the base plate or apparent less settlement is indicated in Winter months. Thus, in reference to the baseline readings taken in July; readings taken in Winter result in a positive difference. Whereas readings taken in August show a negative change due to larger expansion of the riser pipes. Estimated changes in length of the riser pipes due to thermal expansion and contraction are in the order of the observed amplitudes of the cyclic movements. The cyclical movements are out of phase with the temperature and are a result of the thermal expansion and contraction of the freestanding riser pipes. To offset the effect of thermal changes in the riser pipe lengths on settlement observations, the base plate position was selected for reference of extensometer deformation monitoring of the geofoam fill.

Figure 34 shows the top inclinometer profile relative to successive survey elevations of the casing opening. The initial survey and subsequent profiles consistently indicate differential movement of up to 300 mm between the front 20 m and the rear portions of the casing length. The magnitude of the initial misalignment is greater than the cumulative construction and post construction settlements that have occurred over the length of the casing. New compacted fill was placed over the existing embankment as shown in Figure 16. The fill was raised and compacted in thin lifts as geofoam layers were installed. Heavy compaction immediately adjacent to successive top layers of geofoam was taking place as shown in Figure 3. High lateral stresses develop at near surface depths due to compaction (Duncan and Seed, 1986). The coefficient of friction for geofoam interfaces is reasonably high, compared to geomembranes and geotextiles (Sheeley and Negussey, 2000). However, as the density of being very small, the available interface resistance to compaction induced lateral pressures was limited until the pavement surcharge was applied. The top horizontal inclinometer is positioned at layer 8.5. Additional fill placement and compaction occurred above the level and after installation of the inclinometer. The edge of the geofoam fill at 100 South has been displaced outward and the clearance between the fascia panels and the geofoam is much smaller compared to other similar geofoam fills of the I-15 Project. Compaction induced movement or spread took place in the construction phase but before baseline readings were taken. As the load distribution slab was poured and compacted base course was

placed over the geofoam fill, the interface shear resistance between geofoam blocks increased significantly. Further excessive static or transient load induced displacement is not evident in the inclinometer profiles that followed the baseline survey.

5.3. Foundation Settlement Survey

A series of settlement survey points were established along the grade beam at the end of construction on September 24, 2001; as described in Section 4. The survey line extends over both the geofoam and MSE wall sections, Figure 35. Post construction grade beam settlements have reached 25 and 35 mm in the MSE and geofoam fill sections, respectively. The MSE area was surcharged and the segmental fascia panels are tied at different elevations over the wall face. Whereas, each of the geofoam area fascia panels extend over the full height of the wall and are tied to the fill only at the top. The grade beam is continuous and supports the tilt up panel or fascia walls in both the geofoam and MSE sections. As the top inclinometer profile shows, Figure 25, the casing head at the wall face has settled less than the geofoam fill behind the wall. However, post construction observations indicate the grade beam settlement has been larger and is trending to match the adjacent fill settlement profile. The fascia panels in the geofoam area have likely been subjected to down drag loading to result in more settlements of the grade beam, relative to the MSE section. Overall, differential settlements along the grade beam have so far amounted to longitudinal gradient changes of about 0.1 percent.

5.4. Monitoring of Base Level Stresses

Stresses at 100 South continue to be observed with vibrating-wire total earth pressure cells, as described in Section 4. There is one operational base stress cell below the geofoam fill associated with each of the South and North arrays. Readings were taken often for about a year after installation. Thereafter, the leads became inaccessible due to construction activity and were then recovered after almost a year. Figure 36 shows the estimated load history together with stress cell readings over time. Initially, the pressure cells over-registered the base stresses. Subsequent observations indicate the stress cell records generally follow the load history. There was a slight decrease in stress cell readings over about 200 days of no loading during construction. Recent readings in post construction have been decreasing gradually. This may be related to larger post construction settlements taking place below the grade beam, as discussed above. The trend of decreasing stress readings in the more recent data should be explored further with the aid of computer models taking into account the interaction of the fill and fascia panel footing settlements.

6.0 TRENDS AND SIGNIFICANCE OF OBSERVATIONS

The load history and stress cell observations represented in Figure 36 indicate working stress levels are in reasonable agreement with magnitudes anticipated in the design stage. The factored strength working stress level of about 30 kPa was selected to limit settlements to 1 percent strain at the end of construction and to 2 percent in long-term creep over 50 years. Duškov (1997) and Elragi (2000) have shown that the region of linear elastic behavior for geofoam is less than 1 percent strain but this criteria has been used as a reference limit for design. The behavior of small laboratory test samples both in small strain apparent elastic and creep deformation is different from the behavior of full size geofoam blocks (Elragi et al, 2000, Negussey 2002). The geofoam embankment is comprised of large discrete blocks. Seating and gap closure movements that occur in geofoam embankments further complicate direct association of small sample based parameters to prediction of field behavior. Attempts have been made to reconcile field observations and deformation predictions based on laboratory test data (Elragi, 2000;

Stuedlein, 2003). The I-15 instrumentation and monitoring program serves to provide a direct and rational basis of performance confirmation and extrapolation.

Figure 37 presents the global geofoam strain for the South and North extensometer arrays with time. The strains shown include all deformations arising from seating, gap closure and block compression for the full height of geofoam embankment. As the unit weight of geofoam is very small and self weight contributions negligible, a uniform vertical stress state and thus strain state can be assumed over the height of the embankment. Figures 29 and 30 suggest this assumption is reasonable. Along the time line, in Figure 36, construction occurred over a period of 333 days but the rate of loading was not uniform. The accumulated end of construction strains of 0.011 and 0.0097 are in good agreement with the end of construction 1 percent limit strain assumed in design. Over the post construction period to date, further creep strain of about 0.0015 has occurred. If the current deformation trends continue, additional creep strains may be less than 0.015 and 0.02 in post construction 10 and 50 years, respectively. Thus the trend of post construction settlements is consistent with the limit 2 percent global strain in 50 years assumed in design. The work of Srirajan (2001) and Stuedlein (2003) also suggest continuing long-term settlements should remain below 2 percent in 50 years. The trend of post construction settlements at I-15 is consistent with field results reported by Frydenlund and Aabøe (1996) that show post construction geofoam settlements were much less than predicted deformations.

For both the North and South extensometer arrays, the lowest geofoam layer intervals experienced more strain as compared to the relatively uniform strain in overlying geofoam layers. The grade beam restrains the lowest geofoam layer laterally. As a result, the mean normal stress state in the lower geofoam layers would be higher than corresponding states in the overlying geofoam layers. Results reported by Preber et al (1994), Sun (1997) and Anasthas (2001) indicate the modulus of geofoam decreases with confining stress. Under higher confining stress, the trapped air comprising over 95 percent of the geofoam volume becomes more compressed. The larger strain increment associated with the lowest layer of geofoam is consistent with previous results reported from laboratory investigations of geofoam behavior. This observation further suggests that deformation parameters for modeling geofoam under multi axial loading need to consider the effect of confinement. Parameters derived from standard unconfined compression test results can lead to unconservative estimates of deformation when applied to multi axial loading situations.

As noted in the project description, the geofoam embankment at 100 South allowed widening of the roadway over settlement sensitive utility crossings. The geofoam embankment transitions to MSE embankments longitudinally. The previous grade of I-15 along the old alignment was raised with lightweight scoria fill. New compacted soil was placed between the geofoam and the existing embankment. The vertical face of the geofoam embankment is protected by precast fascia panels on grade beam that are tied to the load distribution slab. These different elements interact as components of the roadway. What may be more important is not the absolute magnitude of the geofoam mass settlement but rather the relative movement of the interacting elements and the potential distress that can accrue to affect performance. The scoria, although lightweight in comparison to soil fill, about 1000 kg/m^3 is nonetheless much heavier than geofoam at 18 kg/m^3. The compacted soil density is of the order of 2000 kg/m^3. Observations of the horizontal inclinometer Figure 25 indicate the scoria fill segment is settling less than the geofoam embankment and the intervening compacted fill is serving to moderate the settlement transition between the geofoam and scoria fill areas. The inferred distortion of the top inclinometer profile attributed to compaction induced spreading occurred during construction. Increased interface shear capacity at geofoam layer contacts have developed

with the pavement construction to resist future slumping and lateral displacement under traffic. Continuing observations indicate a general trend towards adjusting relative movements and lower differential settlements.

The grade beam profile shows maximum settlement of 35 mm in the geofoam section and 25 mm in the MSE portions, Figure 35. This differential movement is to date resulting in less than 1/500 distortion but can lead to gradual development of diagonal cracks in facia panels located in the transition area, if present trends continue. The fascia panels rest in the central key way of the grade beam and are thus restricted from lateral movement at the base. At 100 South, the fascia panels are tied into the concrete slab overlying the geofoam fill at the top and are thus restricted from outward movement at the top as well. In previous geofoam installations such as at 3300 South, when the panels were tied to the slab, the connections were noted to strain as the geofoam blocks settled. A design modification that featured a sliding connection was adapted to restrain lateral movement while allowing settlement. This change was not incorporated at 100 South. The geofoam fill settled about 80 mm during construction. In the post construction phase, the grade beam foundation has been settling more than the geofoam foundation and the geofoam fill settlement has been nominal. Again, these are self-adjusting and improvement trends. Down drag on the fascia panels is a likely cause for the greater settlement of the grade beam in the geofoam segment compared to the MSE section as well as perhaps the reduction in post construction stress cell observations, Figure 36. The down drag and bending is also the likely cause for cracks that are now appearing on the fascia panels. Existing distress cracks over the fascia panels should be mapped and further developments should be observed with crack gauges.

Overall, geofoam was the key feature that enabled the I-15 design build project to finish ahead of schedule and under budget. Both in terms of stress and deformation levels, the performance of the geofoam embankments has been satisfactory, as expected. To date, overall geofoam settlements have been and will likely continue to remain well below the foundation settlement. Almost 90 percent of the geofoam settlements occurred during construction.

7.0 SUMMARY

This report presented the data gathered over the construction period and about two years of post construction performance of the 100 South geofoam-widened embankment of the I-15 Reconstruction Project. The project was described in terms of background history, geological setting, instrumentation used, performance observations, and data analysis. Construction settlement records show the geofoam fill continues to perform well in terms of moderating settlements. Stress observations indicate reasonably good agreement with design estimates. Slip connectors were not used to attach the fascia panels to the load distribution slab. Some distress cracking of fascia panels has occurred and should be observed in the future. The trends of post construction observations suggest long-term settlements will remain within tolerable limits, 2 percent strain as assumed in design, over 50 years. As further monitoring continues, the collected body of information regarding long-term deformation and performance verification will be valuable for future projects.

REFERENCES

Anasthas, N., 2001, "Young's Modulus by Bending Tests and Other Engineering Properties of EPS Geofoam", Masters Thesis, Syracuse University, Syracuse, NY

Arai, N., Yokoyama, M., and Tamura, H.; 1996, *"EPS Embankment Construction Road For 32 Ton Dump Trucks At Gassan Dam",* EPS Tokyo '96, Proceedings of the 2nd International Symposium on EPS Construction Method, Tokyo

Bartlett, S., Farnsworth, C., Negussey, D., and Stuedlein, A. W.; 2001, *"Instrumentation and Long-Term Monitoring of Geofoam Embankments, I-15 Reconstruction Project, Salt Lake City, UT",* Proceedings of EPS 2001, 3rd International Conference of EPS Geofoam, Salt Lake City, UT

Boutwell, J. M.; 1933, *"The Salt Lake Region",* Guidebook 17, Excursion C-1, International Geological Congress, XVI Session, United States Government Printing Office, Washington, DC

Brylawski, E., Chua, P. C., and O'Malley, E. S.; 1994, *"Settlement Measurements of 50-ft High Embankments At the Chesapeake and Delaware Canal Bridge",* Proceedings, Vertical and Horizontal Deformations of Foundations and Embankments, Vol. 1, Geotechnical Special Publication No. 40, pp. 398-416; Yeung A. T. and Felio, G. Y., Eds.; ASCE, New York, NY

Cho, A.; 1998; *"Full Speed Ahead",* Engineering News Record, Vol. 241, No. 17, The McGraw Hill Companies, New York, NY

Christensen, C. and Peterson, L. M.; 1996, "Geotechnical Exploration Report, I-15 Corridor Reconstruction Section 4, 600 South", Kleinfelder, Inc, Salt Lake City, UT

Duncan, J. M. and Seed, R. B.; 1986, *"Compaction-Induced Earth Pressures under K0-Conditions",* ASCE Journal of Geotechnical Engineering, Vol. 112, No. 1, New York, NY

Duškov, M.; 1997, *"EPS as a Light-Weight Sub-base Material in Pavement Structures",* Ph.D. Thesis, Delft University of Technology, Delft, The Netherlands

Elragi, A. F.; 2000, *"Selected Engineering Properties and Applications of EPS Geofoam",* Ph.D. Thesis, State University of New York, Syracuse, NY

Elragi, A.F., Negussey, D., and Kyanka, G., 2000, *"Sample Size Effects on the Behavior of EPS Geofoam",* Soft Ground Technology Conference, ASCE Geotechnical Special Publication 112, the Netherlands, May 28 – June 2, 2000

FHWA; 2000, *"Follow-up Review of the Interstate 15 Reconstruction Project in Utah",* Federal Highway Administration, Office of the Inspector General, Audit Report, Report No. IN-2001-007, Washington, DC

Frydenlund, T.E. and Aabøe, R., 1996, *"Expanded Polystyrene – The Light Solution",* Proceeding of the International Symposium on EPS Construction Method, October 29 - 30, Tokyo

Gilbert, G. K.; 1890, *"Lake Bonneville",* U. S. Geological Survey, Monograph 1, Washington, DC

Green, G. E., and Mikkelsen, P. E.; 1988, *"Deformation Measurements with Inclinometers",* Transportation Research Record No. 1169, Transportation Research Board, National Research Council, Washington DC

Hamza, M., Davie, J. R., and Lewis, M. R.; 1994, *"Performance of Three Large Diameter Oil Tanks on Soft Clay",* Proceedings, Vertical and Horizontal Deformations of Foundations and Embankments, Vol. 1, Geotechnical Special Publication No. 40, pp. 398-416; Yeung A. T. and Felio, G. Y., Eds.; ASCE, New York

Hanna, T. H.; 1985, *"Field Instrumentation in Geotechnical Engineering",* Series on Rock and Soil Mechanics, Vol. 10, Trans Tech Publications, Clausthal-Zellerfeld, Germany

Munfakh, G., A., Sarkar, S. K., and Castelli, R. J.; 1983, *"Performance of a Test Embankment Founded on Stone Columns",* Proceedings of the Symposium on Advances in Piling and Ground Treatment for Foundations, Institution of Civil Engineers, London

Negussey, D. 2002. *"Slope Stabilization with Geofoam,"* FHWA Research Project Report, Geofoam Research Center, Syracuse University, Syracuse, NY

O'Rourke, T. D., and O'Donnell, C. J.; 1997, *"Field Behavior of Excavation Stabilized by Deep Soil Mixing",* Journal of Geotechnical and Geoenvironmental Engineering, Vol. 123, No. 6, ASCE, New York

O'Rourke, J. E.; 1978, *"Soil Stress Measurement Experiences",* Journal of Geotechnical Engineering, Vol. 104, No. 12, ASCE, New York

Preber, T., Bang, S.; Chung, Y.; Cho, Y., 1994*,"Behavior of Expanded Polystyrene Blocks",* Transportation Research Board, National Research Council, Washington DC

Sheeley, M., 2000, *"Slope Stabilization Utilizing Geofoam",* Master's Thesis, Syracuse University, Syracuse, NY

Sheeley, M., Negussey, D., 2000, *"An Investigation of Geofoam Interface Strength Behavior",* Soft Ground Technology Conference, ASCE Geotechnical Special Publication 112, the Netherlands, May 28 – June 2, 2000

Ramalho-Ortigao, J. A., Werneck, M. L. G., and Lacerda W. A.; 1983, *"Embankment Failure on Clay Near Rio de Janeiro",* Journal of Geotechnical Engineering, Vol. 109, No. 11, ASCE, New York

Saye, S. R., Esrig, M. I., Williams, J. L., Pilz, J., and Bartlett, S. F.; 2001, *"Lime Cement Columns for the Reconstruction of Interstate 15 in Salt Lake City, Utah",* Foundations and Ground Improvement, Proceedings of Geo-Odyssey 2001, Geotechnical Special Publication No. 113, Brandon, T. L., Ed.; ASCE, New York

Sheeley, M.; 2000, *"Slope Stabilization Utilizing Geofoam",* M.S. Thesis, Syracuse University, Syracuse, NY

Slope Indicator, Inc.; 2002, *"Digitilt Inclinometer Probe",* Bothell, WA

Srirajan, S.; 2001, "Recycled Content and Creep Behavior of EPS Geofoam in Slope Stabilization", M.S. Thesis, Syracuse University, Syracuse, NY

Stokes, W. L.; 1986, *"The Geology of Utah",* Utah Museum of Natural History, University of Utah, and Utah Geological and Mineral Survey, Dept. of Natural Resources, Salt Lake City, UT

Stuedlein, A. W.; 2003, "Instrumentation, Performance and Numerical Modeling of Large Geofoam Embankment Structures", M.S. Thesis, Syracuse University, Syracuse, NY

Sun, M. C.; 1997, "Engineering Behavior of Geofoam (Expanded Polystyrene) and Lateral Earth Pressure Reduction in Substructures", M.S. Thesis, Syracuse University, Syracuse, NY

Warne, R. T., and Downs, D. G.; 1999, *"All Eyes on I-15",* Civil Engineering, American Society of Civil Engineers, Vol. 69, No. 10, Philadelphia, PA

Weiler, W. A., and Kulhawy, F. H.; 1978, *"Behavior of Stress Cells in Soil",* Contract Report B-49(4), to Niagara Mohawk Power Corp., Cornell University, Ithaca, NY

LIST OF FIGURES

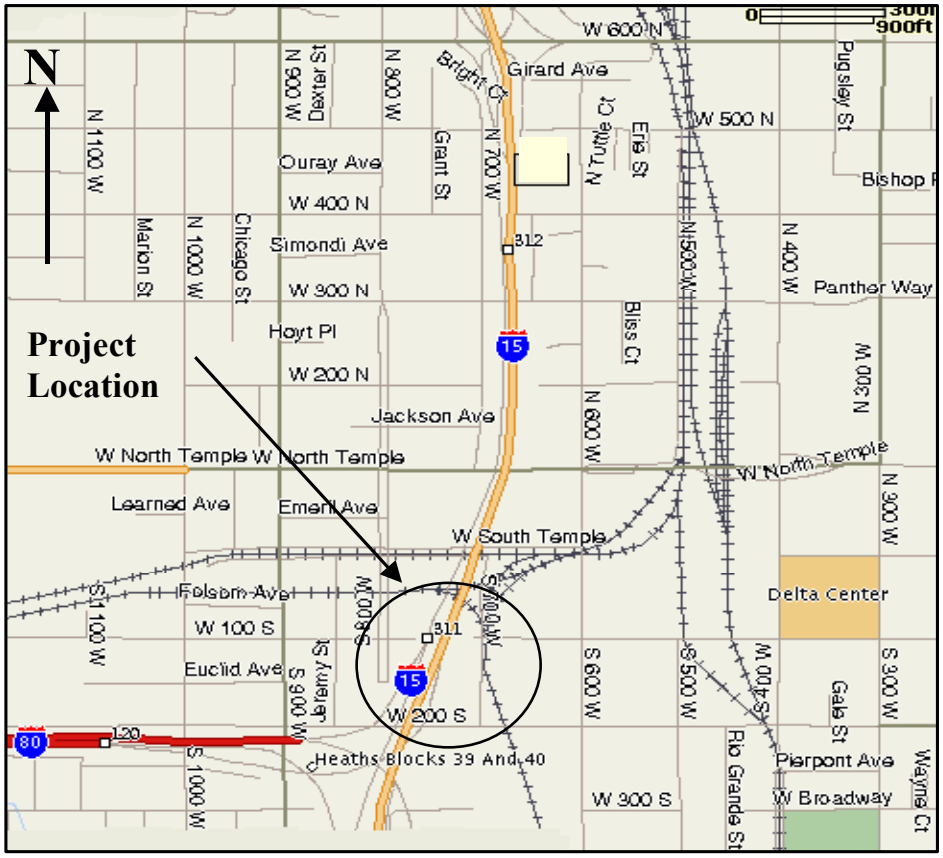

Figure 1 - Project location of 100 South Street and I-15 (Adapted from Mapquest©)

Figure 2 - 100 South Street and I-15. Note soil compaction behind geofoam fill and proximity of road widening to houses and power lines. The fill in the foreground is part of the MSE surcharge.

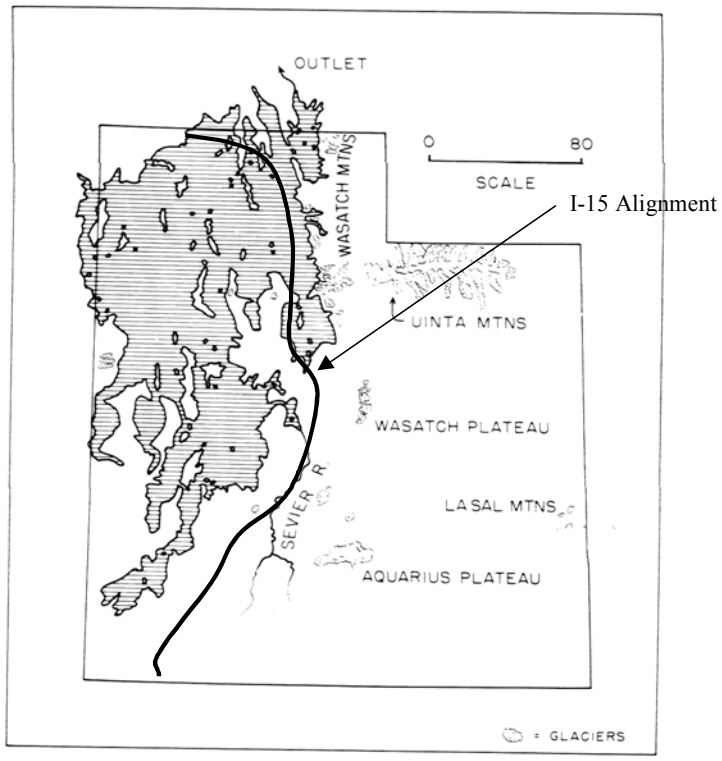

Figure 3 - Lake Bonneville during the late Pleistocene Epoch (Adapted from Stokes 1986).

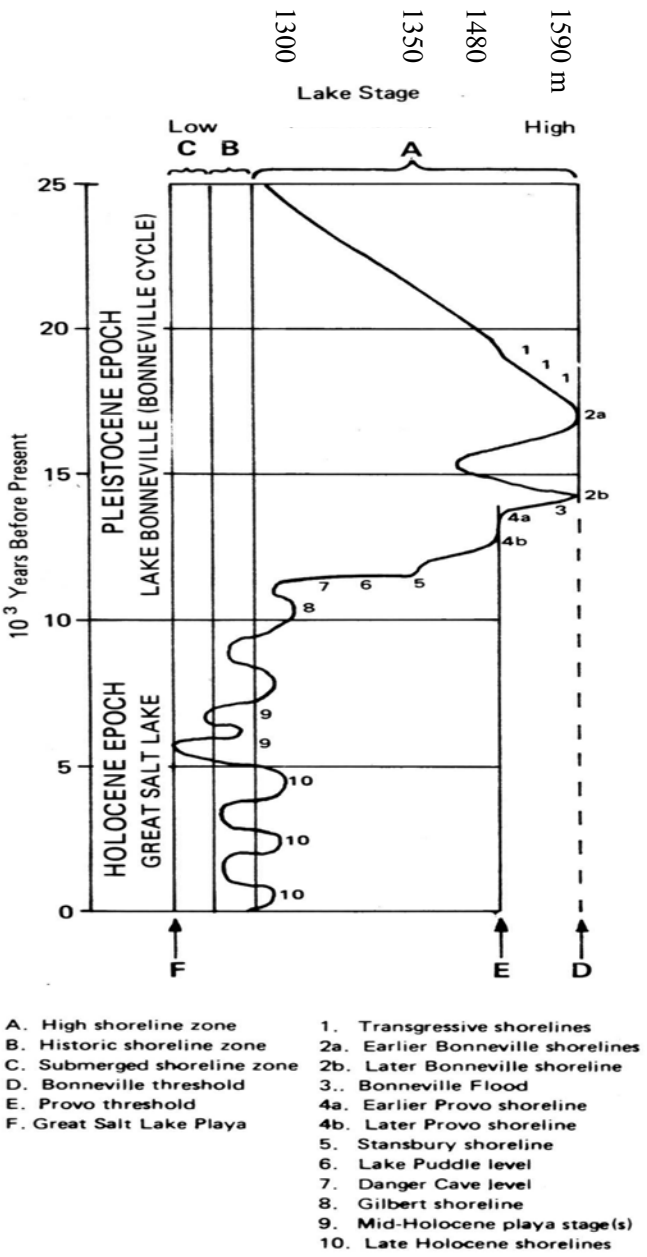

A. High shoreline zone
B. Historic shoreline zone
C. Submerged shoreline zone
D. Bonneville threshold
E. Provo threshold
F. Great Salt Lake Playa

1. Transgressive shorelines
2a. Earlier Bonneville shorelines
2b. Later Bonneville shoreline
3.. Bonneville Flood
4a. Earlier Provo shoreline
4b. Later Provo shoreline
5. Stansbury shoreline
6. Lake Puddle level
7. Danger Cave level
8. Gilbert shoreline
9. Mid-Holocene playa stage(s)
10. Late Holocene shorelines

Figure 4 - Stages of Lake Bonneville to the Great Salt Lake (Adapted from Currey, 1980).

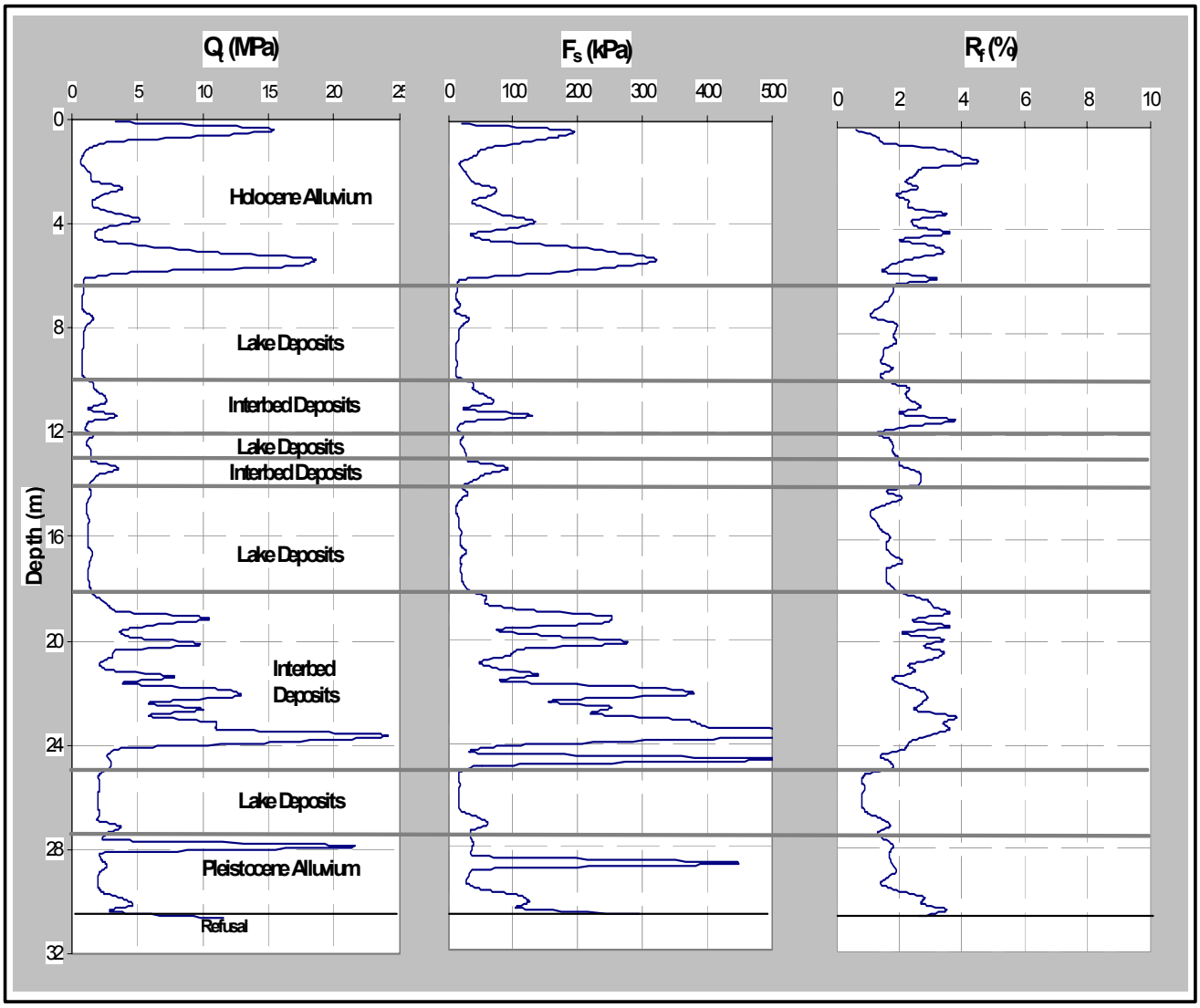

Figure 5 – CPT profile near I-15 and 100 South Street.

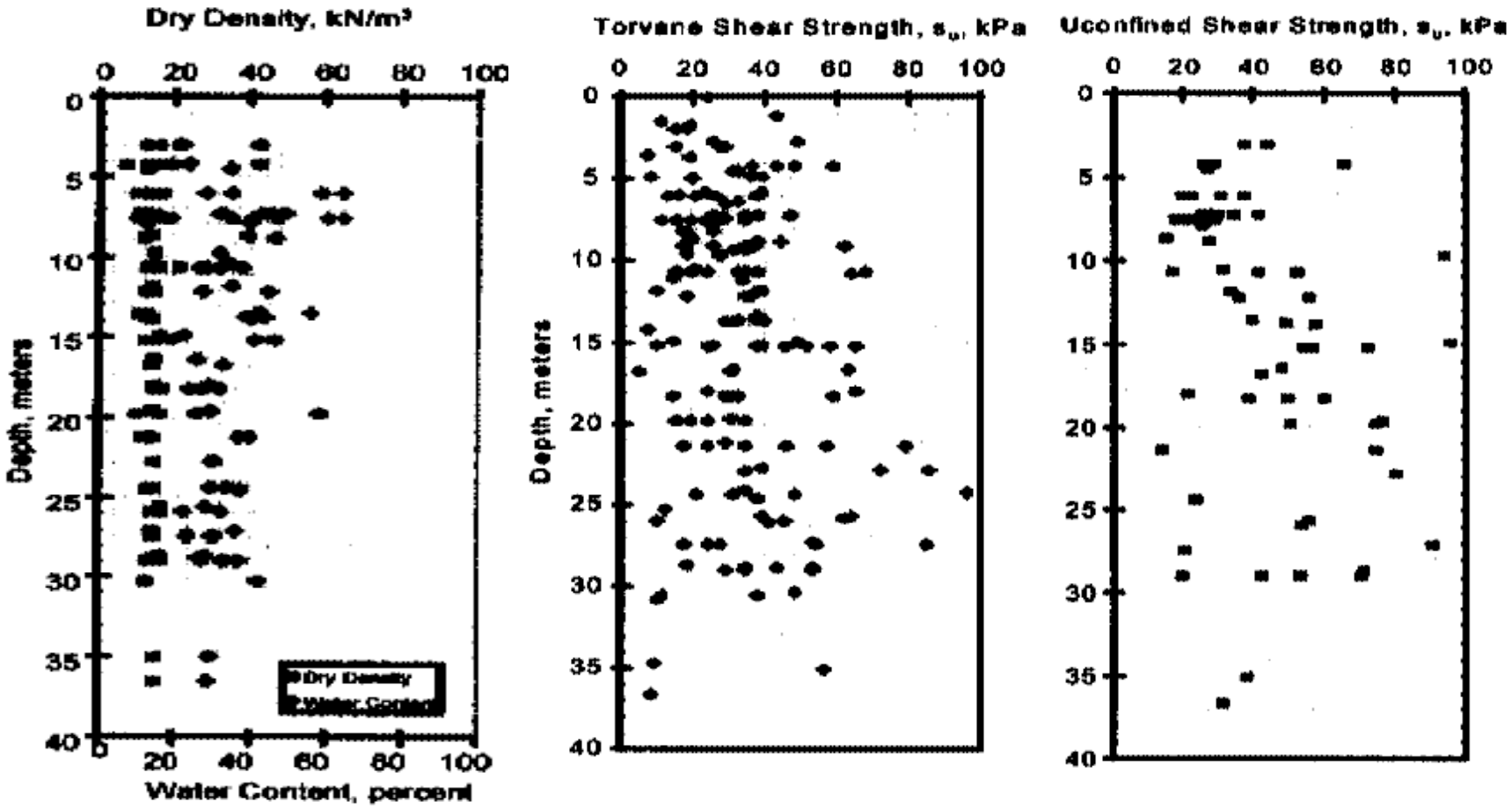

Figure 6 – Water content, density and undrained strength profile near I-15 and 100 South (After Christensen and Petersen, 1996).

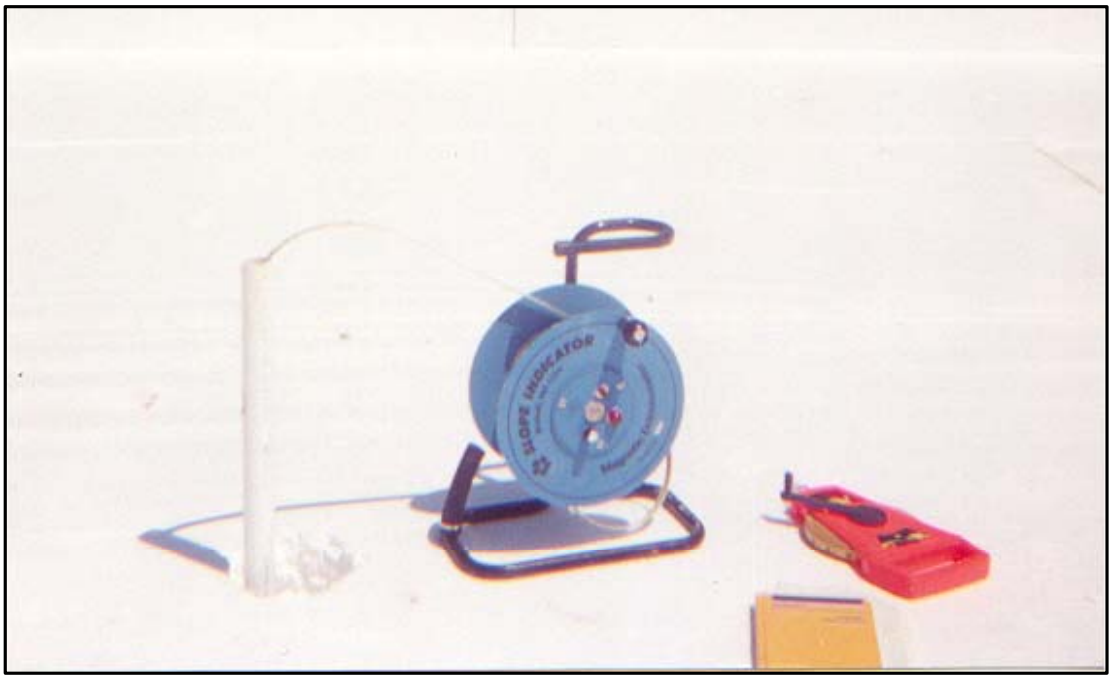

Figure 7 - Magnet extensometer probe inserted in the PVC riser pipe.

Figure 8 - Auguring through a geofoam block at 100 South Street.

Figure 9 – Placement of geofoam block over a riser pipe and magnet plate adjacent to the sand-filled trench and the top horizontal inclinometer.

Figure 10 – Hot wire cutting of a trench into a geofoam block for the top inclinometer casing.

Figure 11 – Completed trench for top inclinometer casing, with plywood forms in foreground. Note the geotextile fabric to retain sand backfill across geofoam block joints.

Figure 12 – Backfilling of top inclinometer casing. Note the foam grout to secure the access head of the casing in the foreground and the small diameter cable return pipe in the foreground.

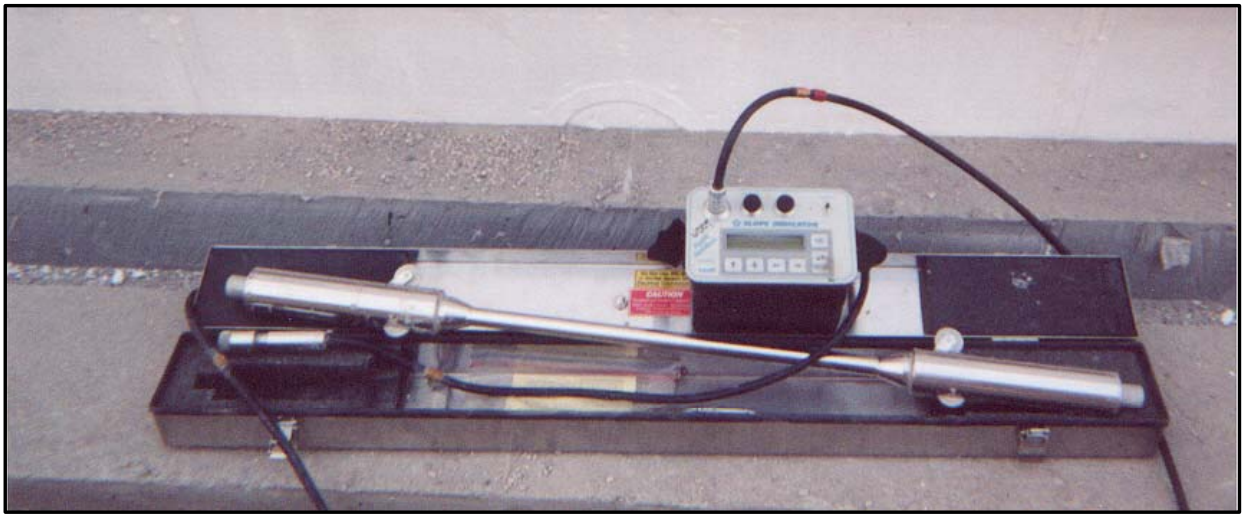

Figure 13 – Horizontal inclinometer probe and readout unit.

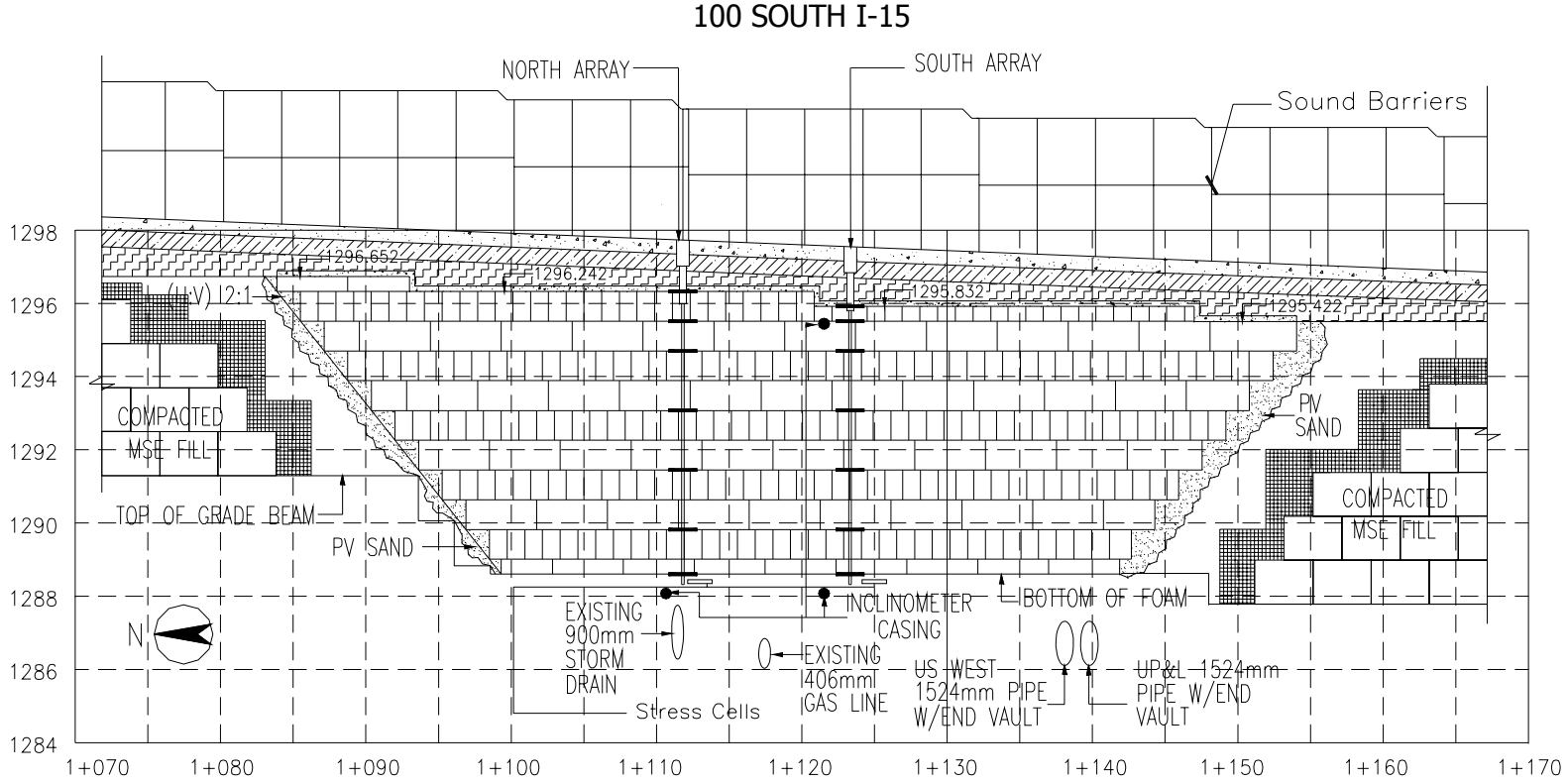

Figure 14 - Profile view of 100 South Street site and instrumentation. Note orthogonal placement of blocks to prevent continuous vertical seams.

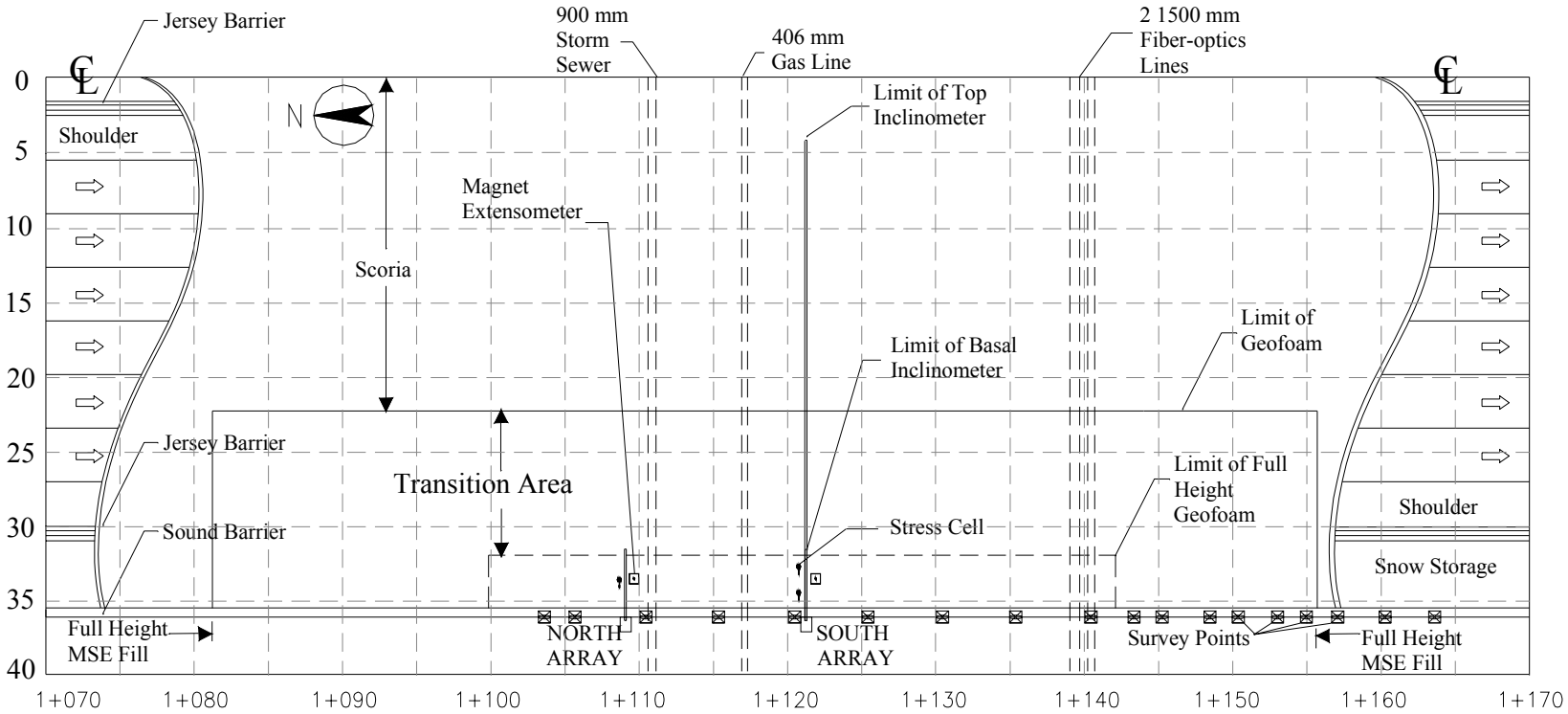

Figure 15 – Plan view of 100 South Street site and instrumentation.

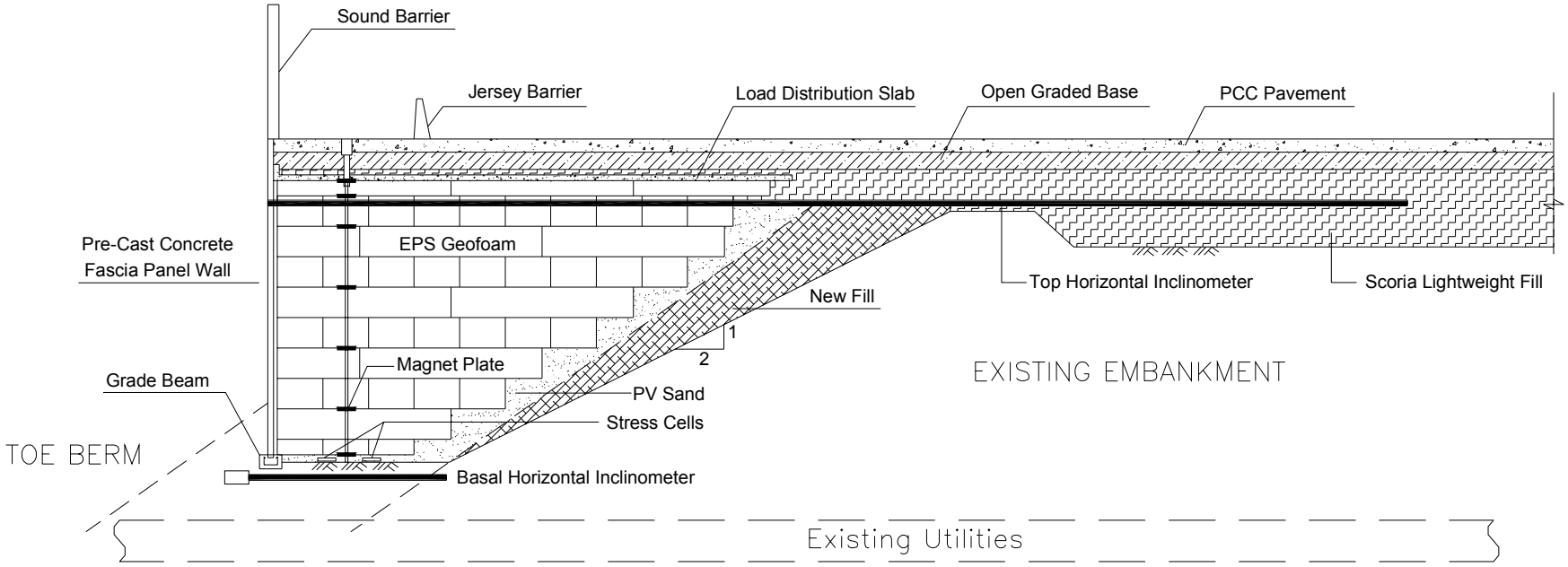

Figure 16 – Section view and instrumentation of the South array.

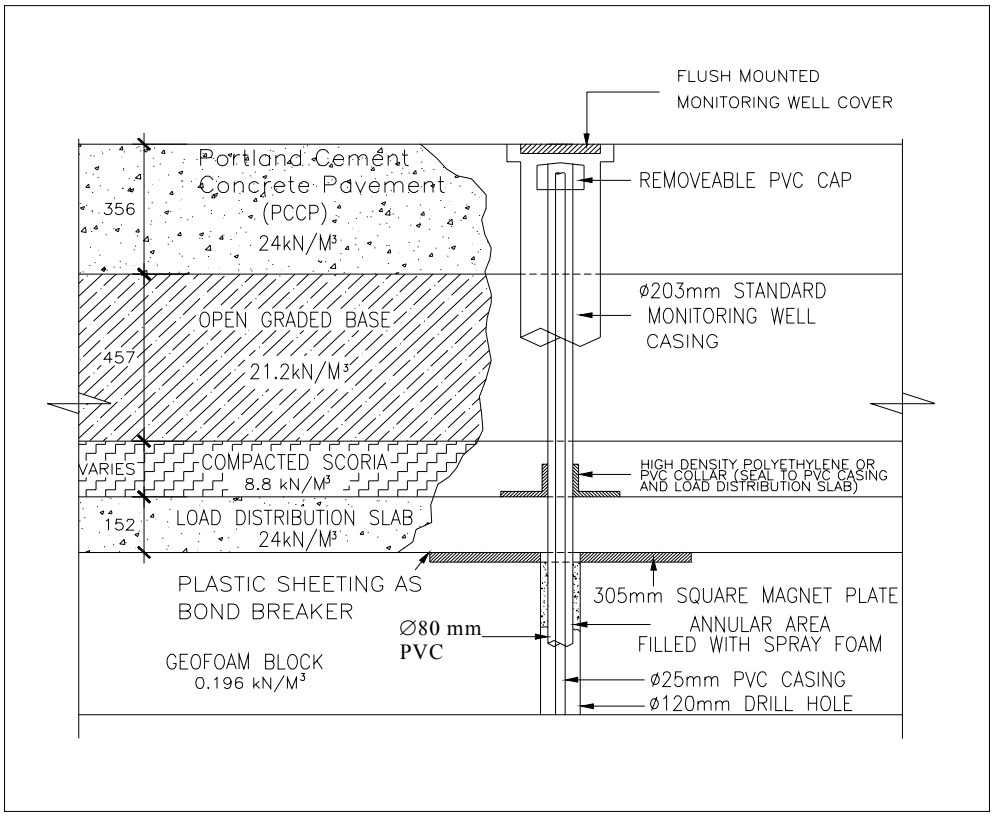

Figure 17 - Magnet extensometer access completion details.

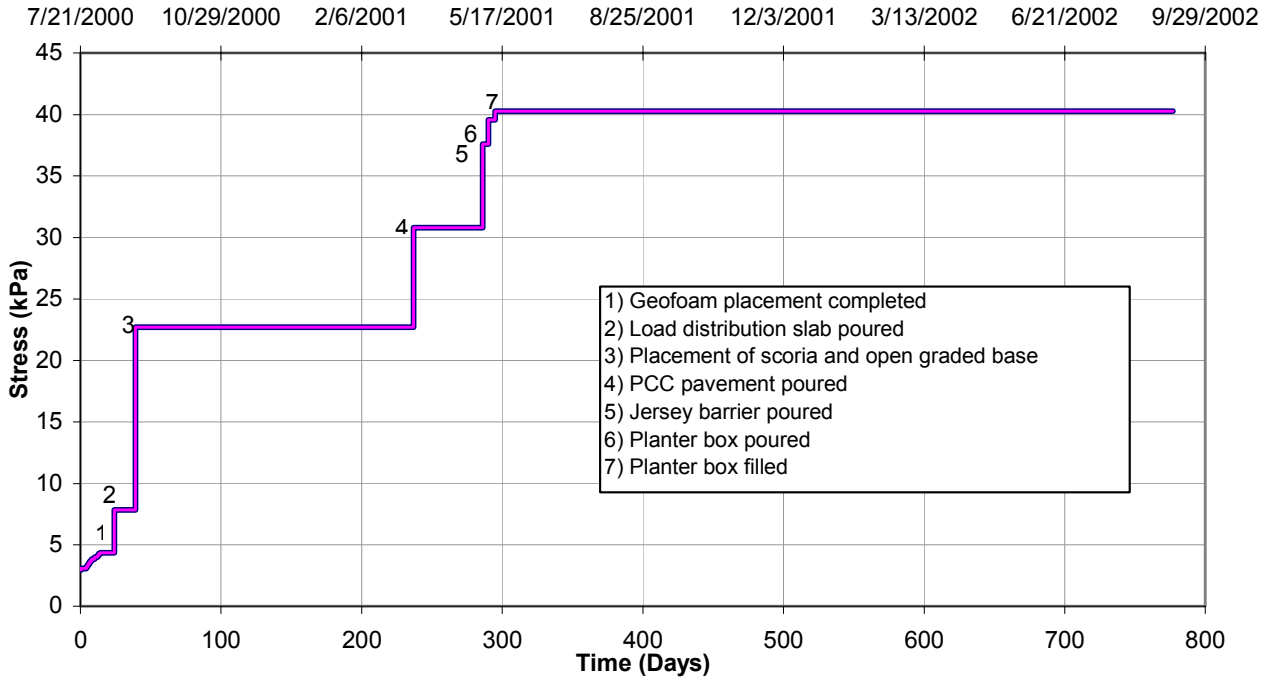

Figure 18 – Estimated load history and construction sequence.

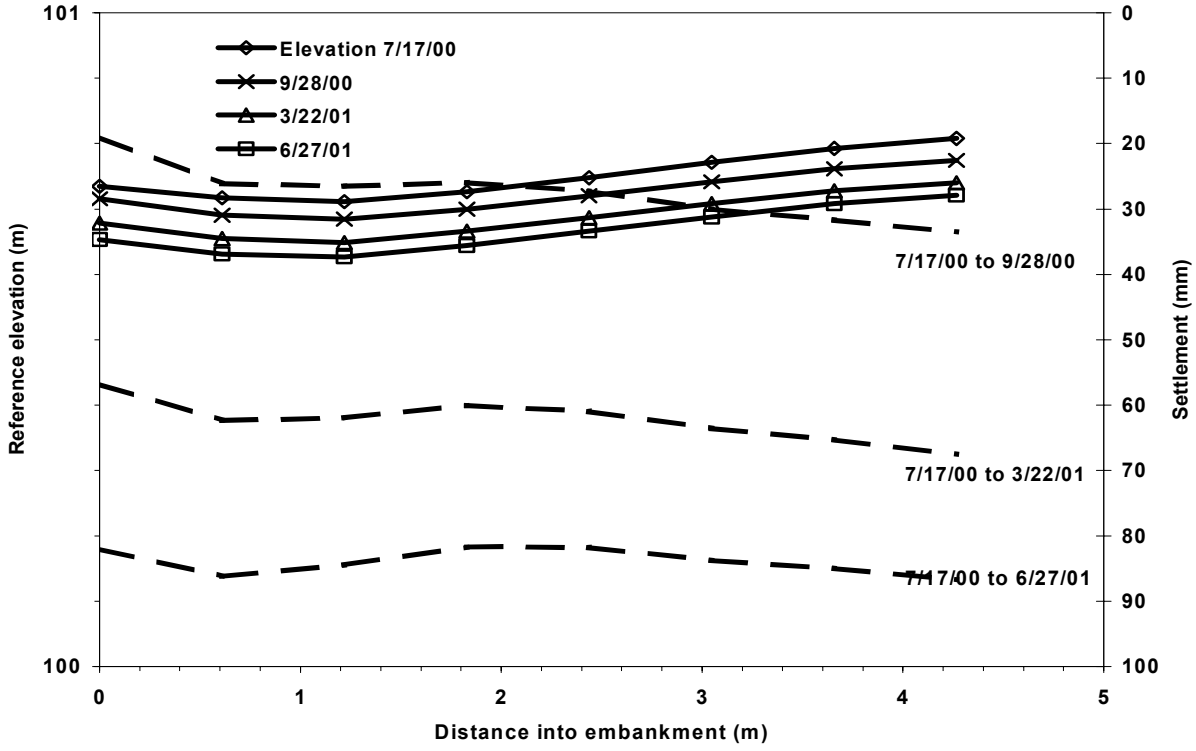

Figure 19 – Base inclinometer settlement profile below the geofoam fill, North array.

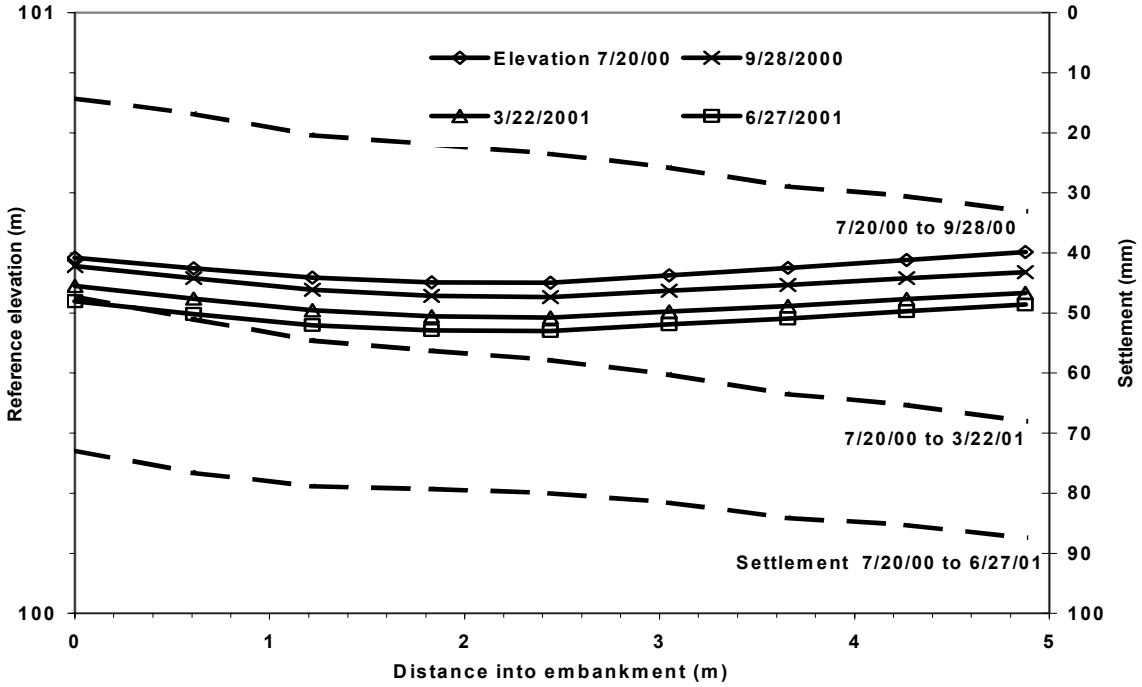

Figure 20 – Base inclinometer settlement profile below the geofoam fill, South array.

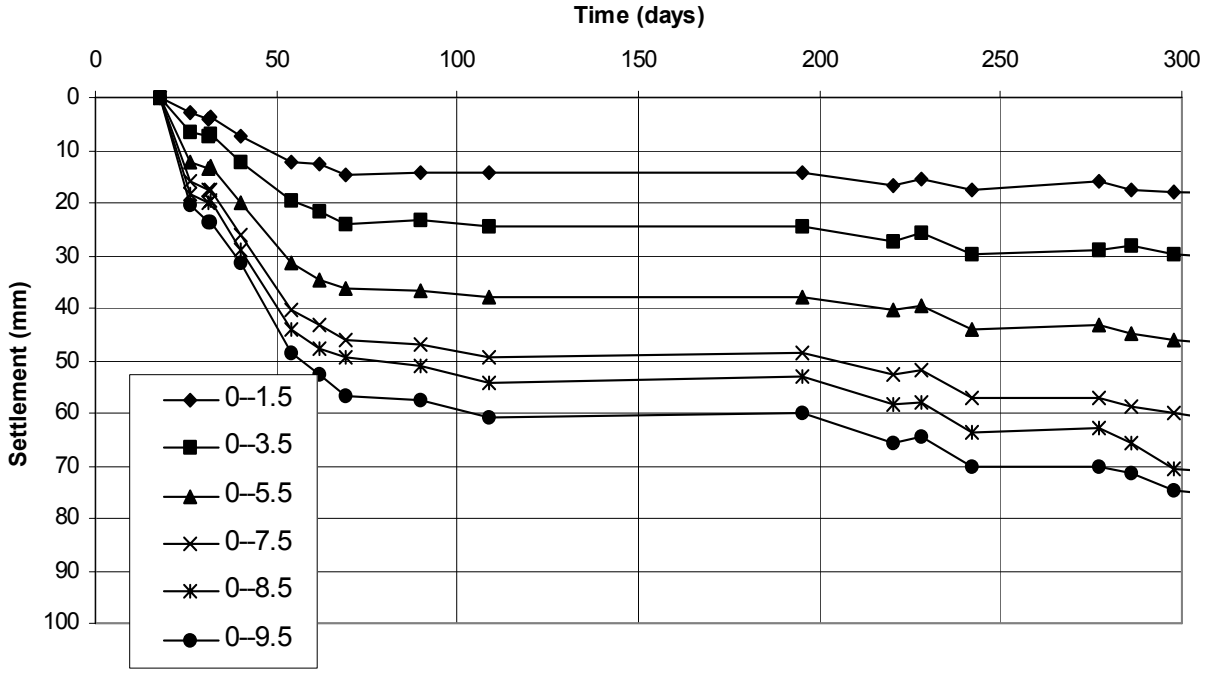

Figure 21 – Cumulative construction stage geofoam layer settlements, magnet extensometers, North Array.

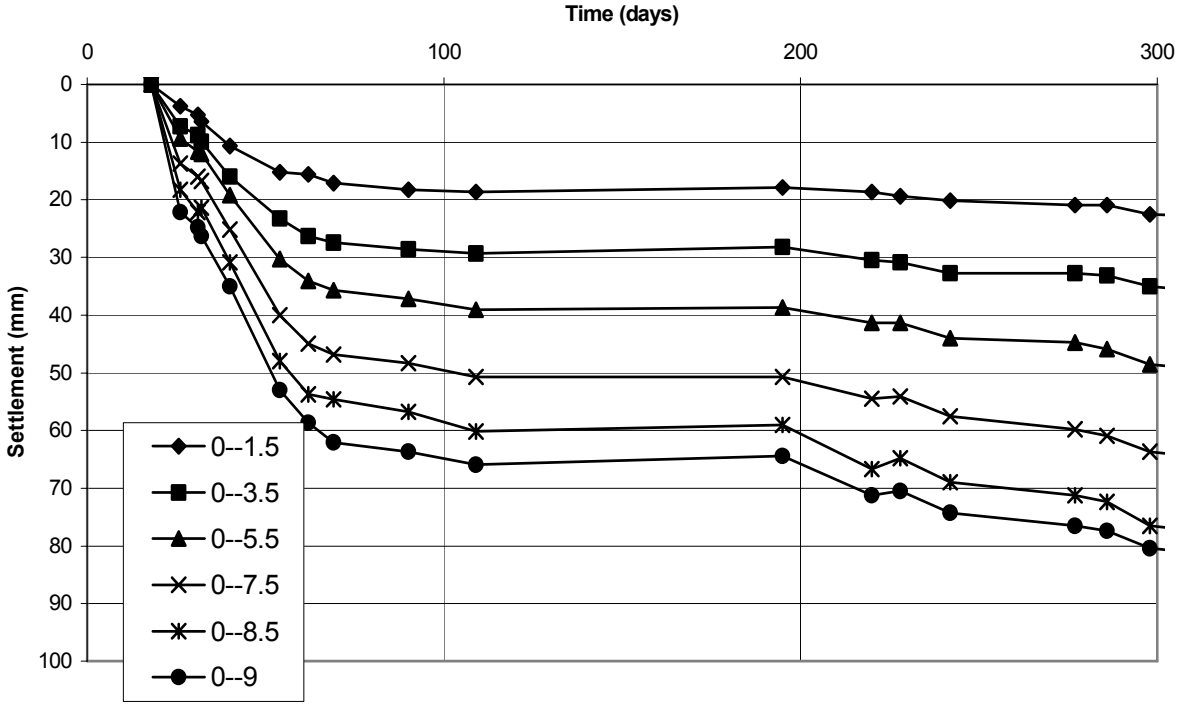

Figure 22 - Cumulative construction stage geofoam layer settlements, magnet extensometers, South Array.

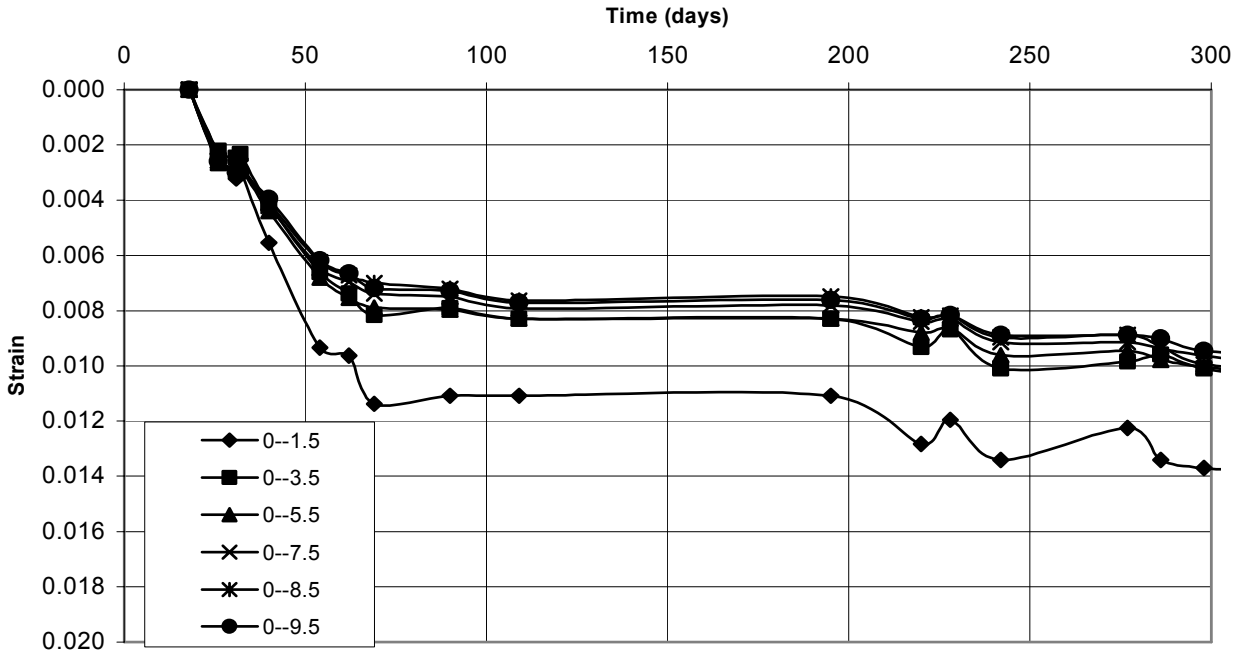

Figure 23 – Cumulative geofoam strain during construction, North array extensometers.

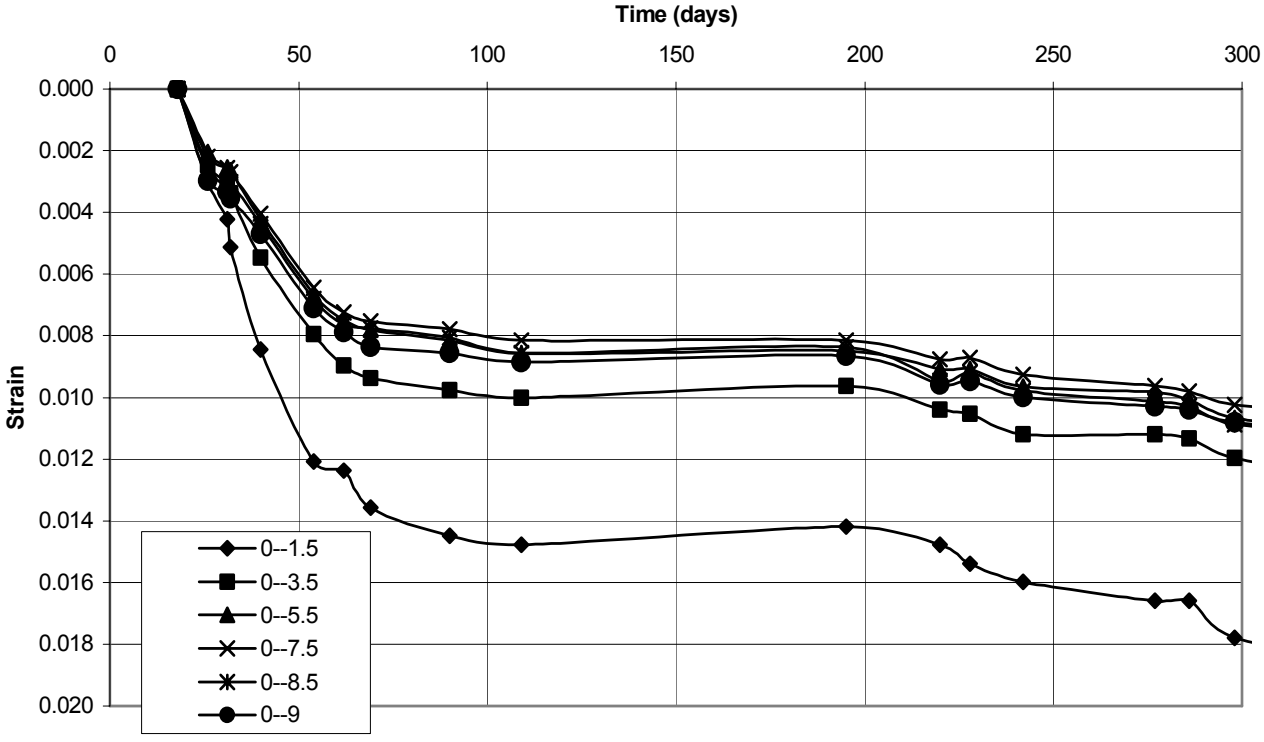

Figure 24 – Cumulative geofoam strain during construction, South array extensometers.

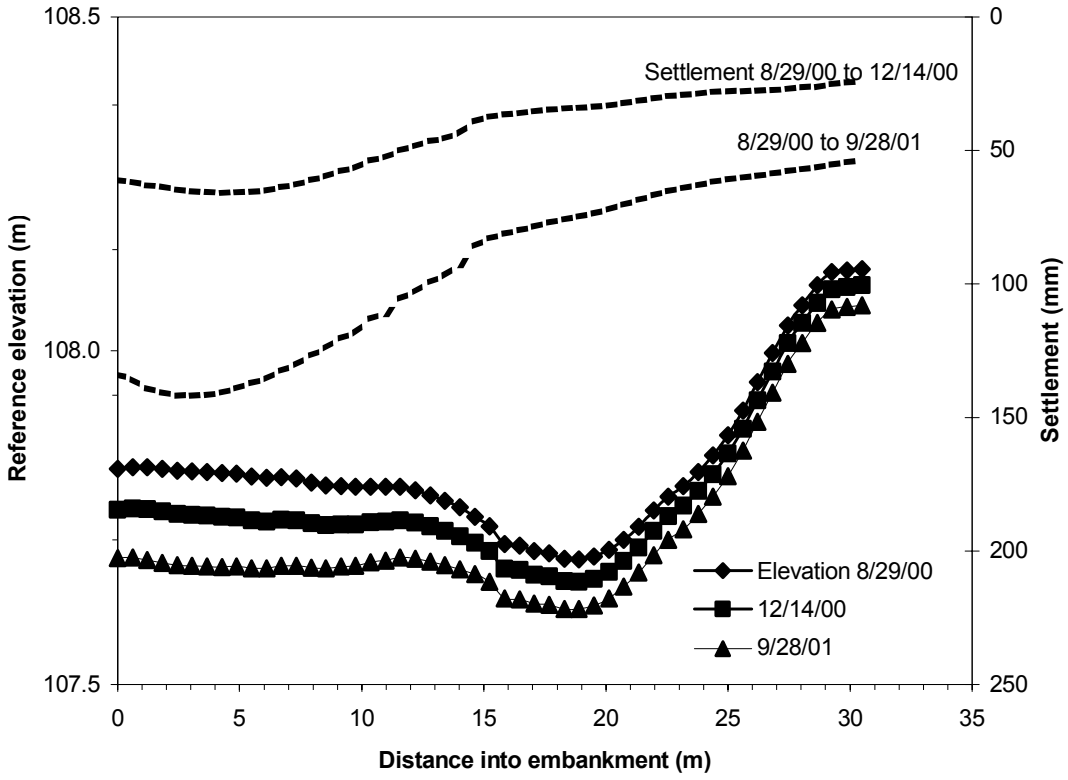

Figure 25 – Top inclinometer construction stage settlement profiles, South array.

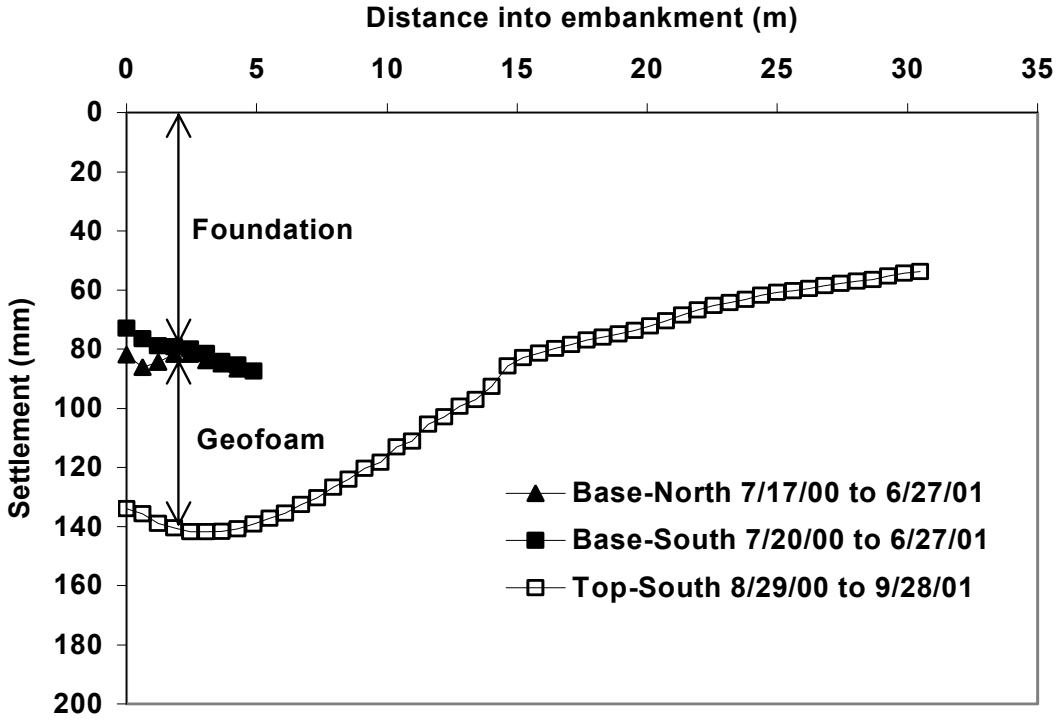

Figure 26 – Base and top inclinometer end of construction settlement profiles, South array

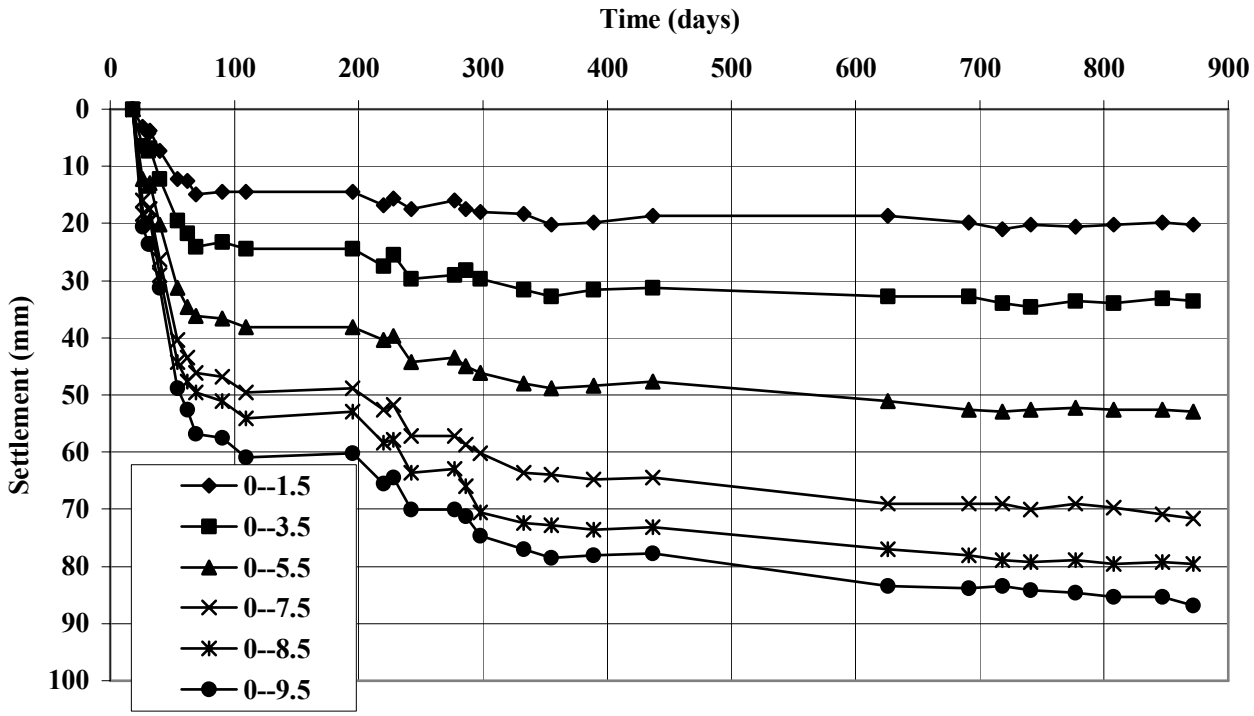

Figure 27 – Cumulative post construction geofoam layer settlements, magnet extensometers, North Array.

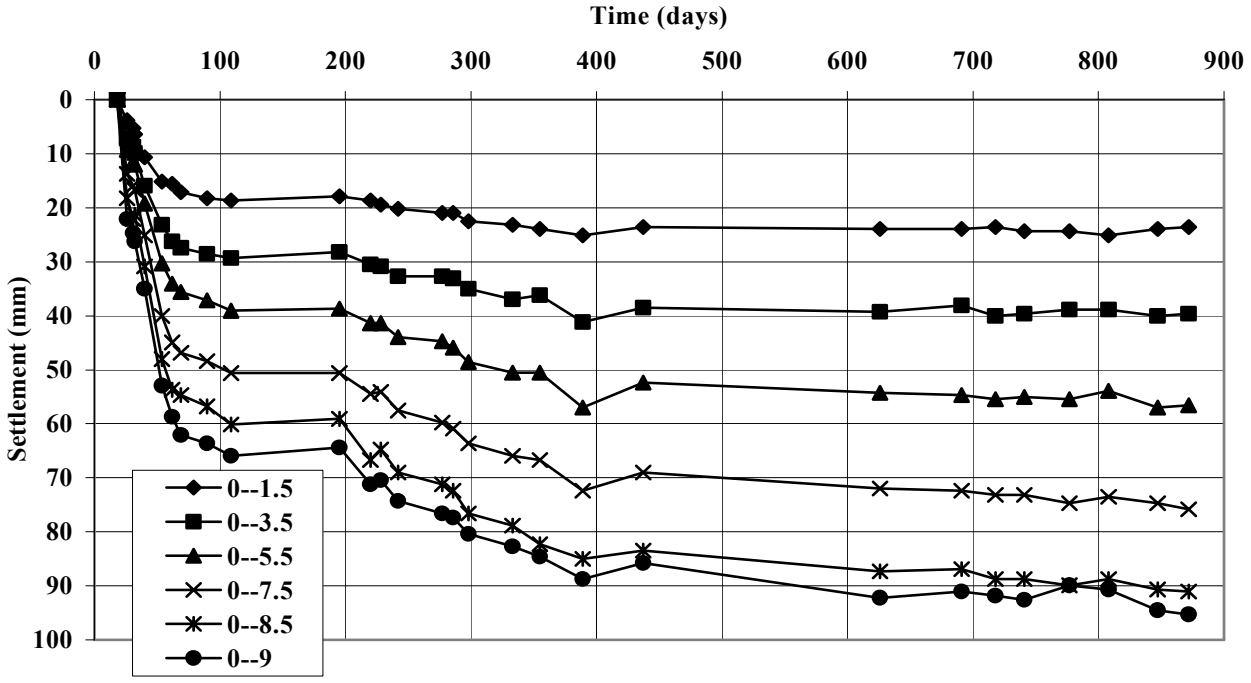

Figure 28 - Cumulative post construction geofoam layer settlements, magnet extensometers, South Array.

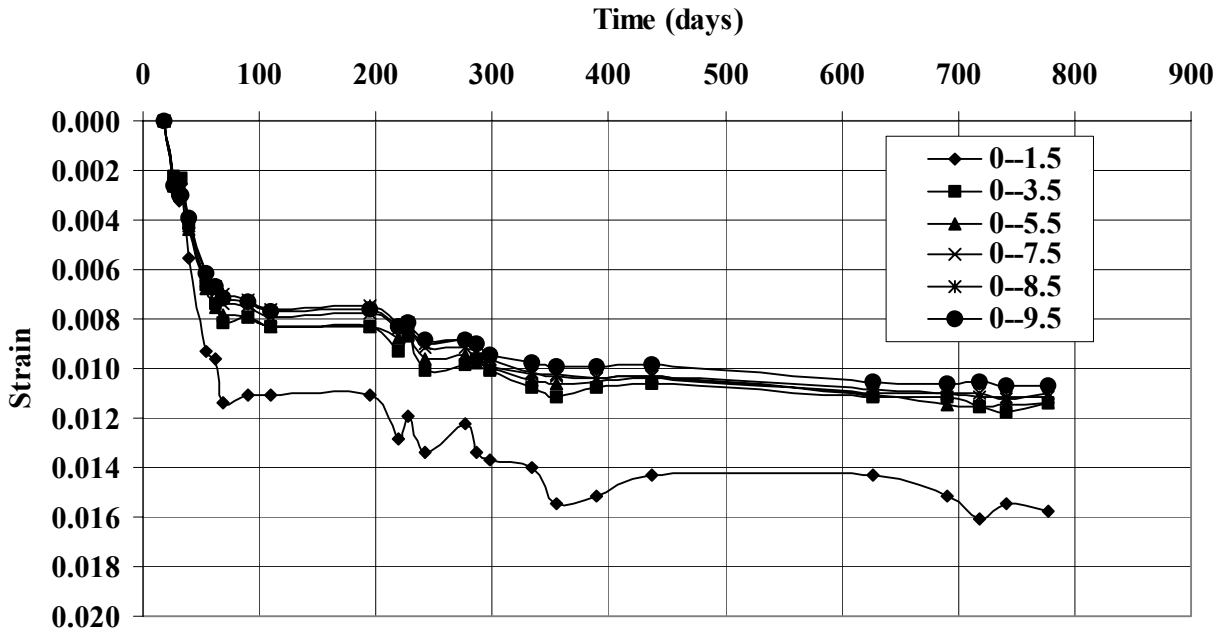

Figure 29 – Cumulative geofoam strain in post construction, North array extensometers.

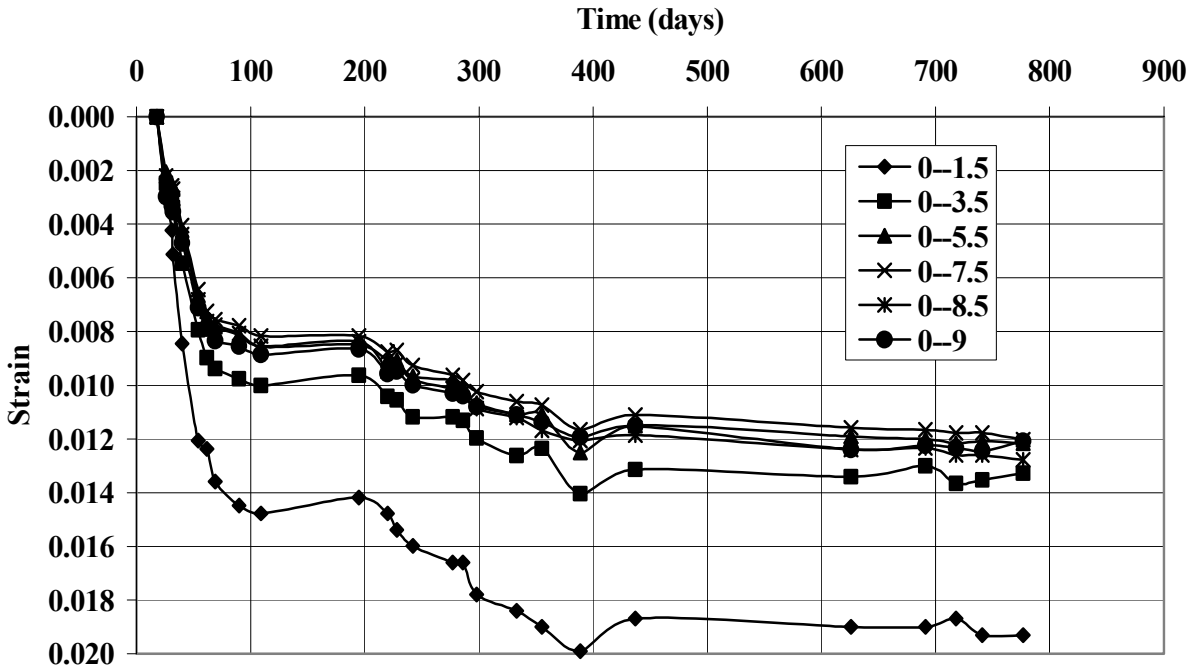

Figure 30 – Cumulative geofoam strain in post construction, South array extensometers.

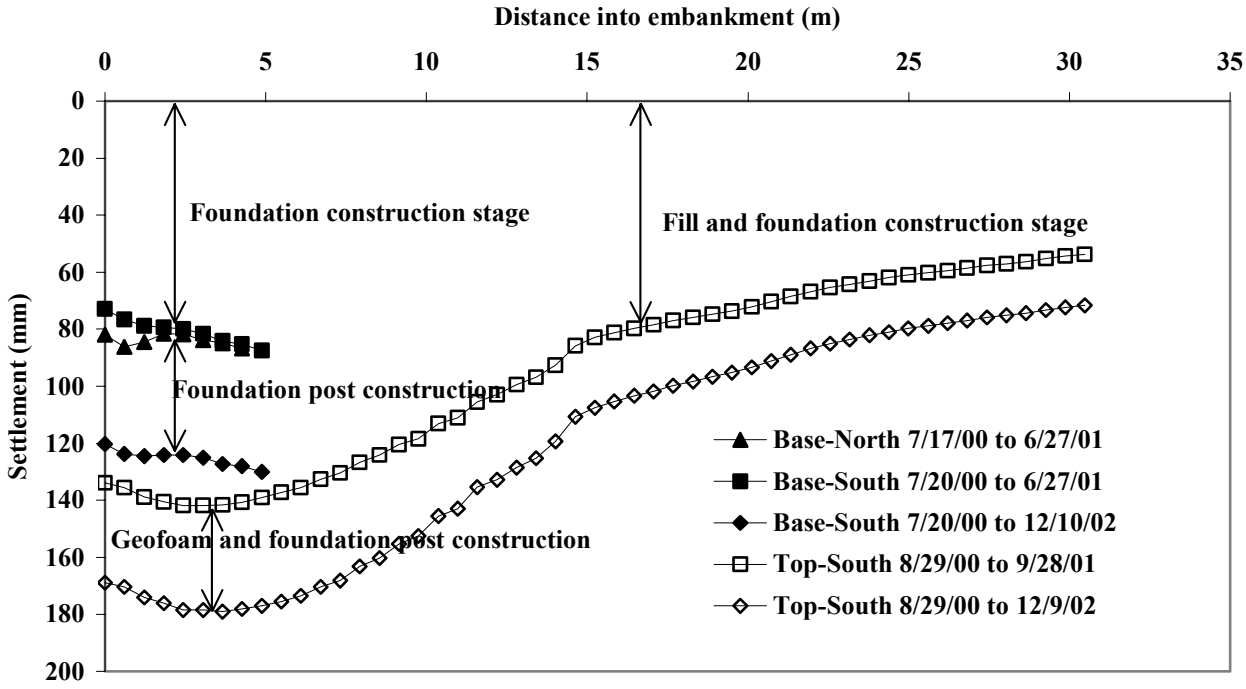

Figure 31 – Base and top inclinometer post construction settlement profiles, South array

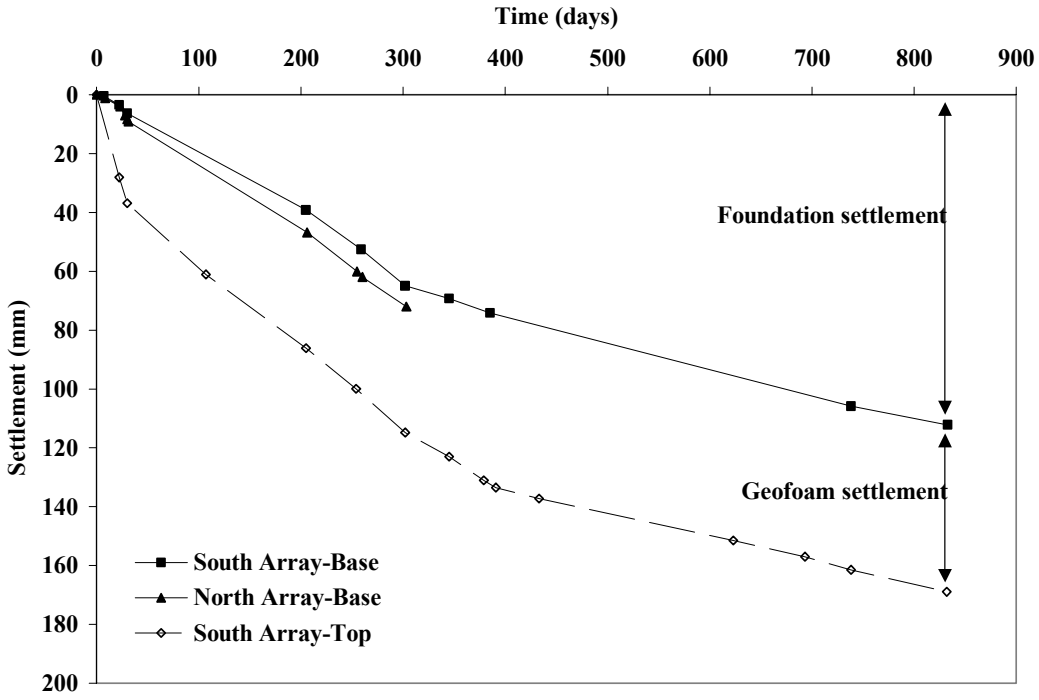

Figure 32 – Settlement estimates based on inclinometer casing head surveys.

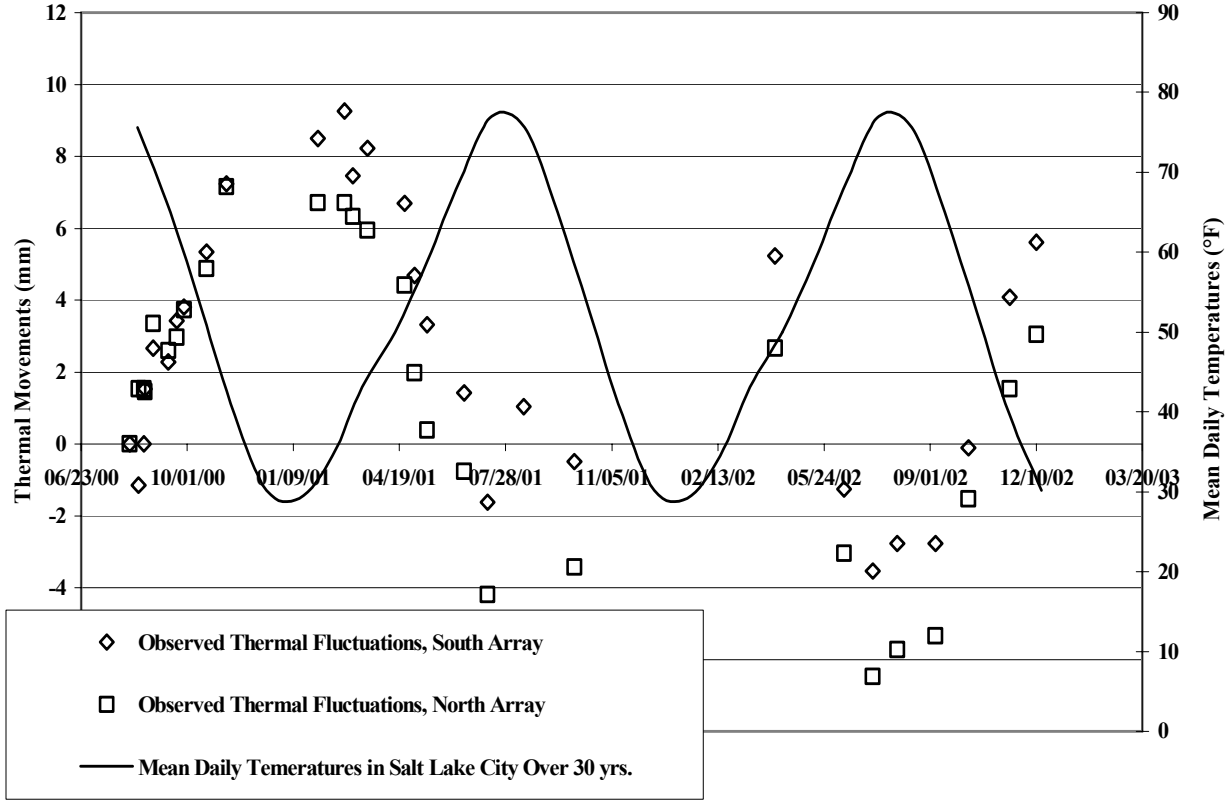

Figure 33 – Seasonal changes in extensometer riser pipe reference lengths.

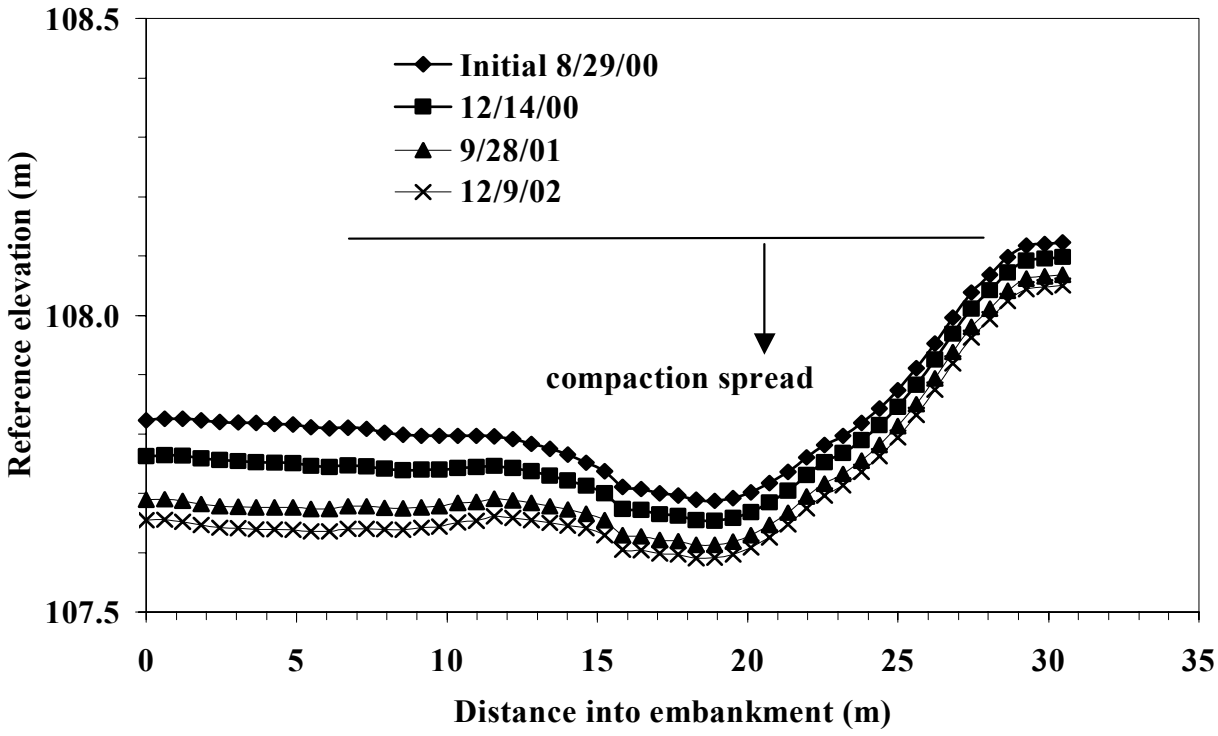

Figure 34 – South array top inclinometer distortion before base line reading.

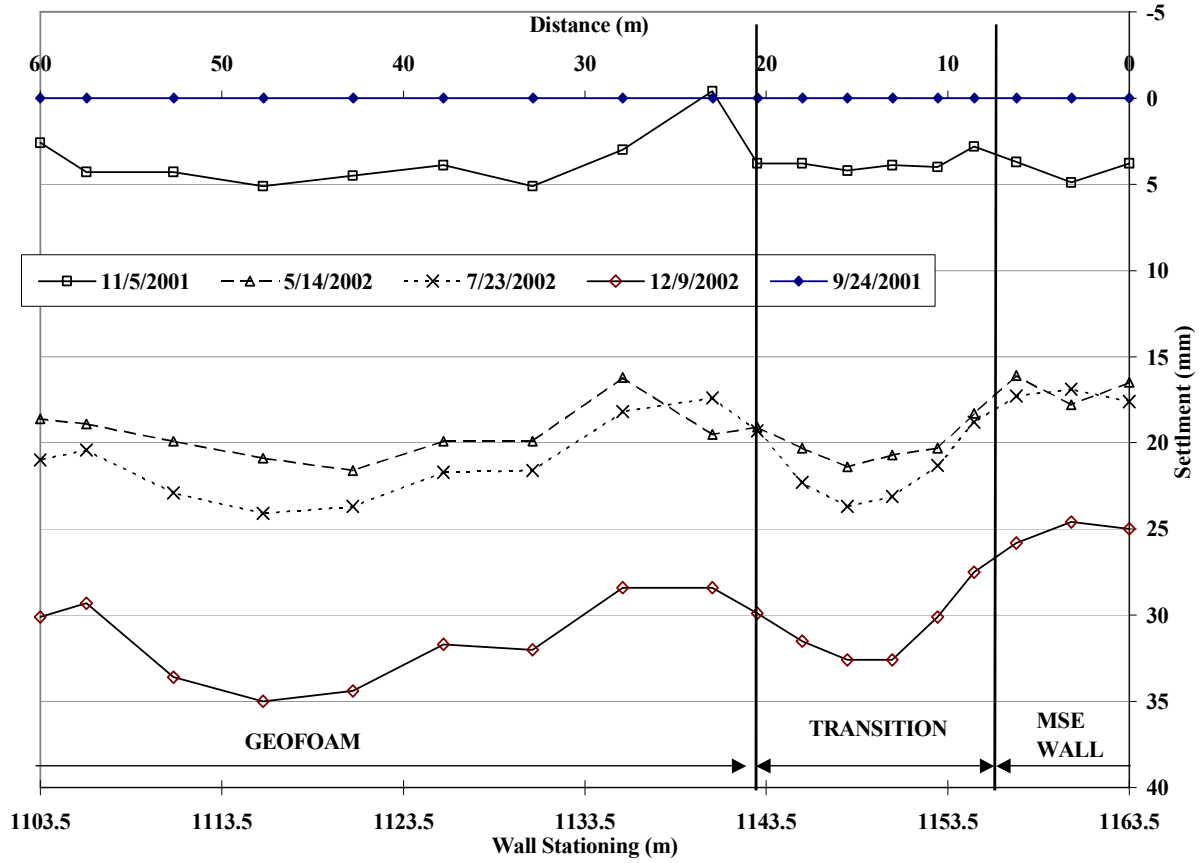

Figure 35 – Grade beam post construction settlement profile

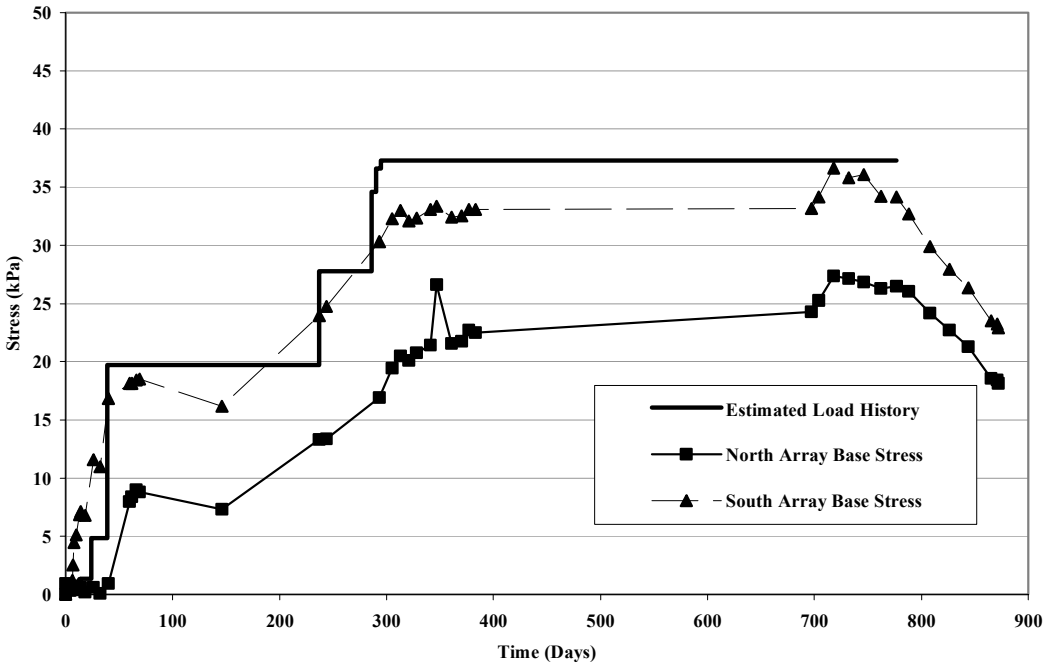

Figure 36 – Estimated load history and base cell pressures at North and South arrays.

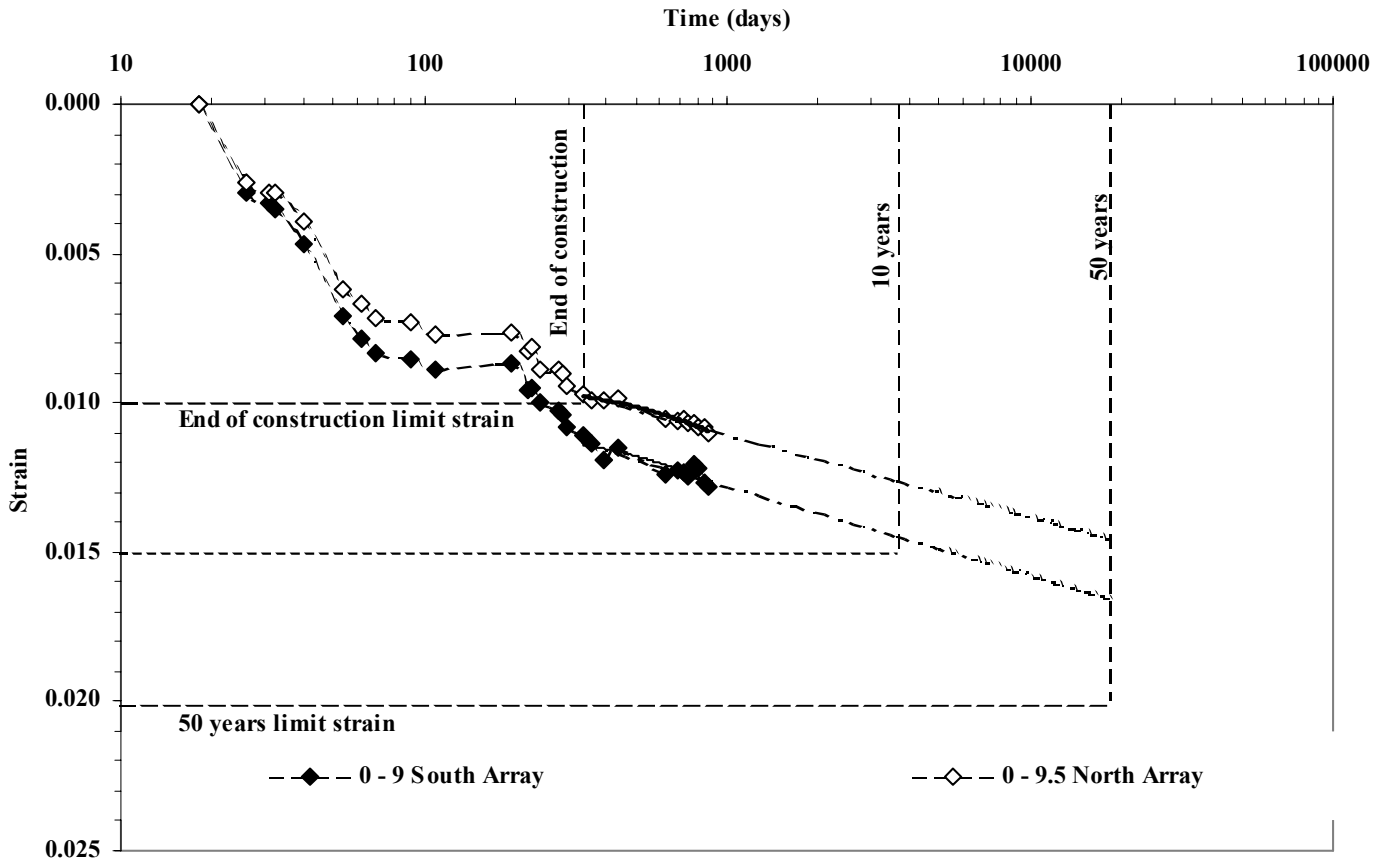

Figure 37 – Projected settlement trend for I-15 geofoam at 100 South.